Pergamon

Journal of Structural Geology, Vol. 16, No. 7, pp. 919 to 940, 1994

0191-8141/94 $07.00+0.00

Extensional origin of ductile fabrics in the Schist Belt, Central Brooks Range, Alaska—II. Microstructural and petrofabric evidence

RICHARD D. LAW

Department of Geological Sciences, Virginia Polytechnic Institute and State University, Blacksburg, VA 24061, U.S.A.

ELIZABETH L. MILLER and TIMOTHY A. LITTLE*

Geology Department, Stanford University, Stanford, CA 94305, U.S.A.

and

JEFFREY LEE†

Department of Earth Sciences, Monash University, Clayton, Victoria 3168, Australia

(*Received* 6 *May* 1992; *accepted in revised form* 13 *September* 1993)

Abstract—A regional system of S-dipping faults is exposed in the Florence and Fall Creeks area of the south-central Brooks Range. This fault system has previously been mapped as the 'root zone' of a N-vergent fold-and-thrust belt of Jurassic–Cretaceous age, although individual faults juxtapose lower grade on higher grade metamorphic rocks suggesting apparent extensional geometries. The structurally highest of these faults places rocks of the oceanic Paleozoic–Mesozoic Angayucham terrane, together with unconformably overlying Cretaceous clastic rocks, on Devonian metagreywacke and phyllite. This metagreywacke–phyllite (MP) unit in turn structurally overlies Devonian (?) and older basement rocks of the Brooks Range Schist Belt along a S-dipping structural contact previously mapped as the Florence Creek fault. The Schist Belt and MP units are both characterized by a regionally developed, S-dipping greenschist facies foliation that displays a pronounced N–S-trending, down-dip elongation lineation which earlier workers regarded as being associated with N-vergent thrusting. While only one foliation (S_d) is recognized in the MP unit, in the underlying Schist Belt this foliation (S_2) overprints an earlier blueschist facies mineral assemblage and associated foliation (S_1).

Mylonites with strong asymmetric crystal fabrics are well developed in quartz stringers in the MP unit and in Schist Belt rocks located at less than 250 m beneath the Florence Creek fault. These asymmetric single- and cross-girdle *c*-axis fabrics indicate a top down-to-the-south shear sense. This shear sense is confirmed in *XZ* sections by the presence of elongate, dynamically recrystallized quartz grains oblique to the S_d–S_2 mylonitic foliation. Quartzose and quartzo-feldspathic lithologies become coarser grained in the deeper levels of the Schist Belt, and a greater proportion of the quartz grains are equant in outline suggesting the increasing importance of temperature-sensitive recovery processes. These deeper level quartz tectonites display less strongly asymmetric cross-girdle *c*-axis fabrics and oblique grain shape alignments for at least a further 7.5 km beneath the fault, the asymmetry still indicating a top-down-to-the-south shear sense. Of the 35 quartz-rich samples selected for detailed microstructural and crystal fabric analysis, only two contain *c*-axis fabrics and oblique grain shape alignments indicating a top-up-to-the-north shear sense.

This pervasive top-down-to-the-south shear sense is inconsistent with tectonite fabrics in the Schist Belt being related to N-vergent thrust faulting, but accords well with an extensional model for exhumation of high-*P* rocks of the Schist Belt. Extension-related high strain fabrics persist for a structural thickness of at least 7.7 km beneath the Florence Creek Fault, indicating that the Florence and Fall Creeks area may be situated over a large-scale (at least 8.0 km thick) zone of extensional shear dipping towards the south. How far this zone of penetrative deformation can be traced along strike remains unclear.

INTRODUCTION

OVER the last decade considerable attention has been focused on the role of extensional deformation in the evolution of orogenic belts (e.g. Platt 1986, Dewey 1988, Molnar & Lyon-Caen 1988, Ratschbacher *et al.* 1989, Hodges & Walker 1992, Malavieille 1993, Wheeler & Butler 1993). In particular the degree to which extension is responsible for the exhumation of high-pressure metamorphic belts still remains a controversial subject (e.g. Platt 1987, 1992, Wheeler 1991, Hsu 1992), and disagreement exists concerning the timing and structural setting of such extension. In the internal zones of orogenic belts this debate is fuelled by the difficulties of distinguishing shortening from extension-related fabrics. Kinematic indicators have, with some success, been used to distinguish between deformation zones associated with thrusting or extension, but the possibility of shear sense reversals due to back-thrusting (retrocharriage or ruckfalten) must always be born in mind unless independent evidence for extensional tectonics, such as

*Current address: Department of Geology, Victoria University of Wellington, P.O. Box 600, Wellington, New Zealand.

†Current address: Division of Geological Sciences, California Institute of Technology, Pasadena, CA 91125, U.S.A.

the juxtaposition of low-grade metamorphic rocks on higher grade rocks, or juxtaposition of stratigraphically younger rocks on older rocks, can also be found. Even then, however, caution must be exercised because there are, at least in principal, many ways to produce younger-over-older relationships that do not involve normal faulting.

For example, Michard *et al.* (1993) have argued that shear sense-dip relationships cannot be used to distinguish normal vs reverse shearing if the shear planes were tilted after the kinematic indicators formed. Similarly, the use of normal-sense metamorphic breaks as evidence for extension relies on the assumption of an earlier undisturbed 'metamorphic stratigraphy' (see reviews by Wheeler 1991 and Michard *et al.* 1993). Likewise, Butler (1984) has demonstrated in the case of the Moine thrust zone of NW Scotland that some of the major thrusts, which display extensional geometries with respect to stratigraphy, since they cut down-section towards the foreland, could be explained by datum-parallel (i.e. horizontal) thrusting of previously hinterland-dipping stratigraphic units (see also Wheeler & Butler 1993, fig. 2).

Clearly, however, the opposite case can also be argued. For example, while accepting that there are many ways to produce younger-over-older relationships that do not involve normal faulting, Hodges & Walker (1992) have argued that regional-scale normal fault relationships are most readily interpreted in terms of extensional tectonics and that alternative tectonic interpretations should carry the burden of proof in such situations. Burchfiel *et al.* (1992) have made a similar case for the development of structures and fabrics exhibiting regional-scale normal-sense geometries in collisional orogens; they have argued that the movement of material in a direction opposite to the principal vergence within an orogenic belt cannot be taken as *a priori* evidence for backthrusting but could also indicate extensional deformation. Wheeler & Butler (1993) have recently argued that hinterland-directed structures throughout the western Alps might be, at least in part, extensional in origin and possibly linked to exhumation of metamorphic complexes.

Debate concerning the role of extension in the evolution of orogenic belts has now begun in Alaska (e.g. Miller & Hudson 1991, 1993, Pavlis *et al.* 1993, Till *et al.* 1993) and much of the attention has focused on the Brooks Range of Arctic Alaska. The Brooks Range (Fig. 1a) represents the northwesternmost continuation of the Mesozoic–Early Cenozoic foreland fold and thrust belt of the North American Cordillera. North-directed thrust faulting in the Brooks Range, which began in Middle Jurassic time (Wilber *et al.* 1987, Mayfield *et al.* 1988) is interpreted to have resulted in 500–800 km shortening of a Paleozoic to Early Jurassic continental shelf sequence (Oldow *et al.* 1987, Mayfield *et al.* 1988, Grantz *et al.* 1991). The interior and deeper-seated portions of this orogen underwent deformation under blueschist-facies conditions during this event. These high-pressure rocks, which are widely exposed in

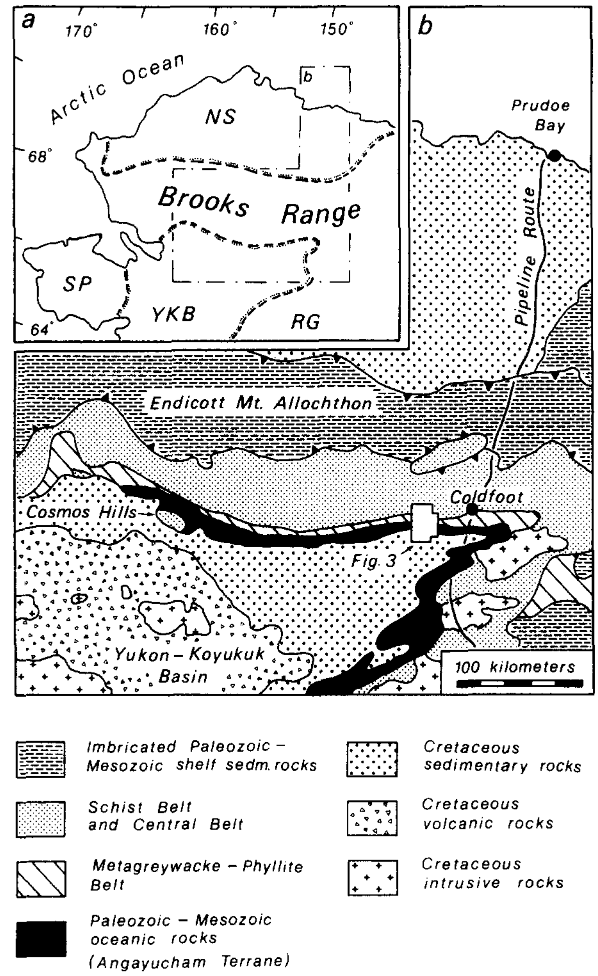

Fig. 1. Location maps. (a) Major geologic and topographic provinces in northern Alaska. NS = North Slope, SP = Seward Peninsula, YKB = Yukon–Koyukuk basin, RG = Ruby Geanticline. (b) Generalized geology of the central Brooks Range and adjacent areas. Location of the Florence and Fall Creeks study area is indicated by box.

the Schist Belt along the southern flank of the Brooks Range, have been pervasively retrogressed and strongly overprinted by a younger deformational fabric (Little *et al.* 1994) developed parallel to a regional system of S-dipping faults. This system of S-dipping faults has traditionally been interpreted as an Alpine-style root zone (e.g. Mull *et al.* 1987, Dillon 1989).

However, problems associated with thrust-related models for the evolution of the internal zone of the Brooks Range include (Little *et al.* 1994): (1) contacts previously mapped as N-vergent thrusts place very low-grade metamorphic rocks on top of higher grade schists, including blueschists; (2) the dominant metamorphic fabric in the Schist Belt is a greenschist-facies schistosity (S_2) that overprints rare crenulated relicts of blueschist-facies minerals; (3) kinematic indicators in D_2-deformed tectonites of the Schist Belt are not N-vergent, but are predominantly top-down-to-the-south; and (4) mid-Cretaceous K–Ar and $^{40}Ar/^{39}Ar$ cooling ages of white mica from the Schist Belt rocks overlap with the deposition age of the Yukon–Koyukuk basin located immediately to the south of, and derived in part from erosion of, the Schist Belt (Fig. 1b). The Yukon–Koyukuk basin was developed on attenuated crust of the Brooks Range orogen's metamorphic hinterland (e.g. Miller & Hudson 1991). These geologic relationships seem most easily explained by crustal extension, rather than thrust-related deformational processes.

This companion paper to Little *et al.* (1994) reports on microstructural and petrofabric data from a suite of more than 150 oriented samples collected in a 165 km^2 region along the southern flank of the Brooks Range, and provides key data for the interpretation of mapped fabrics being related to top-down-to-the-south shear. These two studies build on previous work by the Alaska Division of Geological and Geophysical Surveys (e.g. Dillon *et al.* 1981, 1986, 1987, Mull *et al.* 1987) and are the first studies to systematically investigate the possibility that widespread metamorphic fabrics in the Brooks Range might be related to top-down-to-the-south extension, rather than top-up-to-the-north thrusting. This is the most detailed quartz fabric study reported to date from the Brooks Range, and brings into question the current interpretation (e.g. Gottschalk 1990) of the widespread penetrative metamorphic fabrics exposed along the southern flank of the range being chiefly thrust related. These new data suggest that extensional overprinting of earlier formed blueschist-facies fabrics is more pervasive than previously thought, and that most of the measurable ductile strain in these rocks is a consequence of N–S stretching in association with top-down-to-the-south extensional shear.

GEOLOGICAL AND STRUCTURAL FRAMEWORK

The southern Brooks Range of Arctic Alaska (Fig. 1a) consists of a series of S-dipping tectonic units that are progressively less metamorphosed to the south. The southernmost of these units, the Angayucham Terrane (Fig. 1b), is composed of oceanic rocks of Devonian to Jurassic age (e.g. Bird 1977, Dillon *et al.* 1981, Jones *et al.* 1988) which have been regionally metamorphosed in the prehnite–pumpellyite facies (e.g. Dusel-Bacon *et al.* 1989). These oceanic rocks are unconformably overlain to the south by a thick section of Cretaceous (Aptian–Albian) conglomerate and sandstone (Dillon 1989). To the north, the Angayucham terrane lies in fault contact above a thin panel of low-grade (greenschist) metagreywackes and phyllite that, in one locality, has yielded Devonian palynomorphs (Gottschalk 1987, Murphy & Patton 1988). This metagreywacke–phyllite (MP) unit is, in turn, underlain to the north by the Brooks Range Schist Belt (Fig. 1b).

The Schist Belt consists of multiply deformed and metamorphosed pelitic and quartzose schists, with lesser mafic to silicic metavolcanic rocks and calcareous schists (e.g. Brosge & Reiser 1971, Nelson & Gryback 1980, Dillon *et al.* 1986, Little *et al.* 1994) and is thought to range from late Proterozoic to Late Devonian in age (e.g. Dillon *et al.* 1980, Hitzman *et al.* 1986, Armstrong *et al.* 1986). In the south-central Brooks Range, the contact between the MP unit and the underlying Schist Belt has been interpreted as a structural contact (e.g. Gottschalk 1987, Till *et al.* 1988, Dusel-Bacon *et al.* 1989) referred to as the Florence Creek Fault, although the increase in penetrative deformation of both the MP unit and the underlying Schist Belt rocks towards the contact suggests (Little *et al.* 1994) that, at least in some areas, the contact may be a shear zone rather than a discrete fault surface.

The southernmost part of the Schist Belt together with the immediately overlying MP unit are characterized by a well developed E–W-striking foliation and S-plunging stretching lineation that has been assumed to be associated with crustal thickening during northward directed overthrusting during the Jurassic–Cretaceous part of the Brookian Orogeny (e.g. Dillon *et al.* 1987). Similarly the system of S-dipping faults that overlie the Schist Belt and bound the Angayucham terrane along the southern flank of the Brooks Range has traditionally been interpreted as an Alpine-style root zone for the thrust faults (e.g. Mull *et al.* 1987, Dillon 1989).

Several recent studies have questioned this earlier interpretation, suggesting that the S-dipping fault system may have extensional (i.e. top down-to-the-south) rather than thrust displacement (e.g. Box 1987, Miller 1987, Gottschalk & Oldow 1988, Christiansen 1989, Ave Lallement *et al.* 1989, Gottschalk *et al.* 1990, Miller & Hudson 1991, Miller *et al.* 1990a,b, Oldow *et al.* 1991). However, while agreeing that the faults may be extensional, many workers (e.g. Gottschalk 1987, 1990 and Till & Moore 1991 in the Coldfoot area of the south-central Brooks Range) (Fig. 1) have argued that the regional S-dipping dominant foliation and lineation within the Schist Belt are associated with earlier thrust-related deformation.

In contrast, in the Florence and Fall Creeks area (Fig. 1b) of the south-central Brooks Range, detailed structural evidence for widespread penetrative deformation and metamorphism associated with an extensional event has been reported by Little *et al.* (1994). In this companion paper, we present supporting microstructural and quartz *c*-axis fabric data from quartz-rich lithologies in both the Schist Belt and overlying MP unit for crystal-plastic deformation associated with top-down-to-the-south extensional shear in the Florence and Fall Creeks area.

ANALYTICAL TECHNIQUES AND DATA PRESENTATION

Two shear-sense indicators were particularly useful in distinguishing between crystal-plastic deformation associated with reverse (top-up-to-the-north) and normal (top-down-to-the-south) motion in quartz-rich lithologies of both the Schist Belt and the overlying MP unit. These shear-sense indicators (Fig. 2) are: (1) obliquity between foliation and preferred shape alignment (S_B) of elongate dynamically recrystallized quartz grains; and (2) asymmetry of quartz *c*-axis fabrics with respect to foliation and lineation.

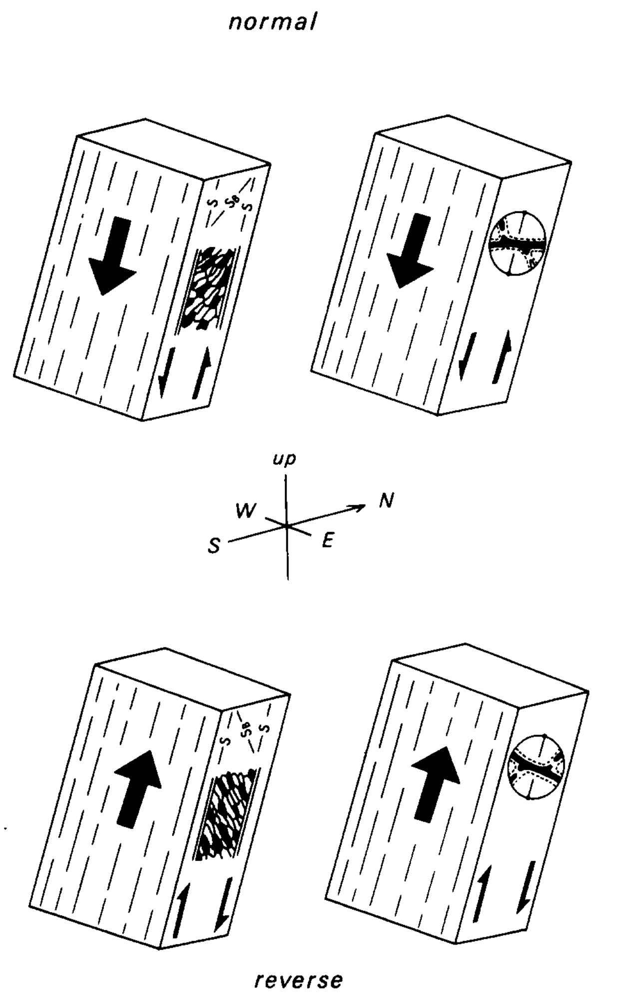

Fig. 2. Microstructural and crystal fabric shear-sense indicators used to distinguish between normal (top-down-to-the-south) and reverse (top-up-to-the-north) displacement. Microstructure: obliquity between penetrative foliation (S) and preferred alignment (S_B) of elongate dynamically recrystallized quartz grains. Crystal fabric: sense of asymmetry of quartz c-axis fabrics. Both microstructures and crystal fabrics viewed towards the west on planes oriented parallel to lineation and perpendicular to foliation.

In this paper all microstructural and crystal fabric data are presented on section planes oriented perpendicular to the foliation (XY) and parallel to the stretching lineation (X). In all figures, these XZ section planes are, in a geographic sense, viewed towards the W. Thirty-five of the most quartz-rich samples from the Schist Belt and overlying MP unit were selected for detailed microstructural and petrofabric analysis. Sample locations are shown in Fig. 3.

The estimated distance (d) of individual samples from the projected position of the Florence Creek fault are given in Table 1. These distances were estimated using the dip-parallel cross-section drawn through the study area by Little *et al.* (1994, fig. 4) and were measured perpendicular to the projected fault surface.

Petrofabric analyses of quartz c-axis preferred orientation were carried out on one XZ thin section from each sample using an optical microscope and universal stage; a general minimum of *ca* 700 c-axis were measured in each section. The c-axis data are presented on equal-area, lower-hemisphere, spherical projections whose plane of projection contains the grain shape lineation (X) and pole (Z) to foliation; in all these projections the foliation is vertical and lineation within the foliation is horizontal. The c-axis plots were contoured using the computer program developed by Starkey (1989). Details of the contouring procedure used are given by Starkey (1977).

MICROSTRUCTURAL SHEAR-SENSE INDICATORS IN THE SCHIST BELT

The Schist Belt lies beneath the Florence Creek fault and is composed of a series of pelites and metaquartzites intercalated with metamorphosed andesite and greenstone (Fig. 3). No original detrital features have been observed within these plastically deformed and recrystallized schistose rocks. Little *et al.* (1994) have demonstrated that the schists are polydeformed, locally retaining evidence for at least one earlier schistosity (S_1) that pre-dates the dominant S-dipping foliation (S_2). Where D_2 strain is lower, compositional layering in the schists is subparallel to S_1, a domainal foliation defined by thin quartzose laminae, micaceous folia and quartz veinlets. This foliation is everywhere plicated by tight to isoclinal crenulations and transposed into parallelism with S_2. In the most highly strained and/or most recrystallized rocks, only the younger foliation, S_2, is evident. Little *et al.* (1994) have demonstrated that this D_2 deformation was accompanied by a greenschist-facies metamorphic overprint.

Thirty-two samples from the Schist Belt were selected for combined microstructural and crystal fabric analysis. All selected samples were taken from quartz-rich horizons, displaying a strongly developed E–W-striking foliation and S-plunging grain shape lineation lying within the foliation. Each selected sample displays, in thin section, a single foliation defined by elongate quartzose or phyllosilicate-rich domains. We emphasize that all analyzed samples were collected from outcrops displaying a single, homogeneously developed, penetrative foliation equivalent to S_2 of Little *et al.* (1994). No reported samples were collected from discrete shear zones such as the late stage shear bands described by Little *et al.* (1994, fig. 5c) or from rocks where S_1 is locally preserved. The kinematic interpretation of an individual sample is therefore regarded as being valid up to at least the scale of the outcrop from which it was taken.

Oblique grain-shape alignments in quartz-rich domains

Quartz-rich domains are characterized by preferred alignment of the long axes of elongate, dynamically recrystallized quartz grains in 22 of the 32 samples selected for detailed analysis. In XY thin sections, the preferred grain shape alignment is oblique to the foliation (Fig. 4). This grain shape alignment will be referred to as S_B following the nomenclature of Law *et al.* (1984). For the samples analyzed, the obliquity be-

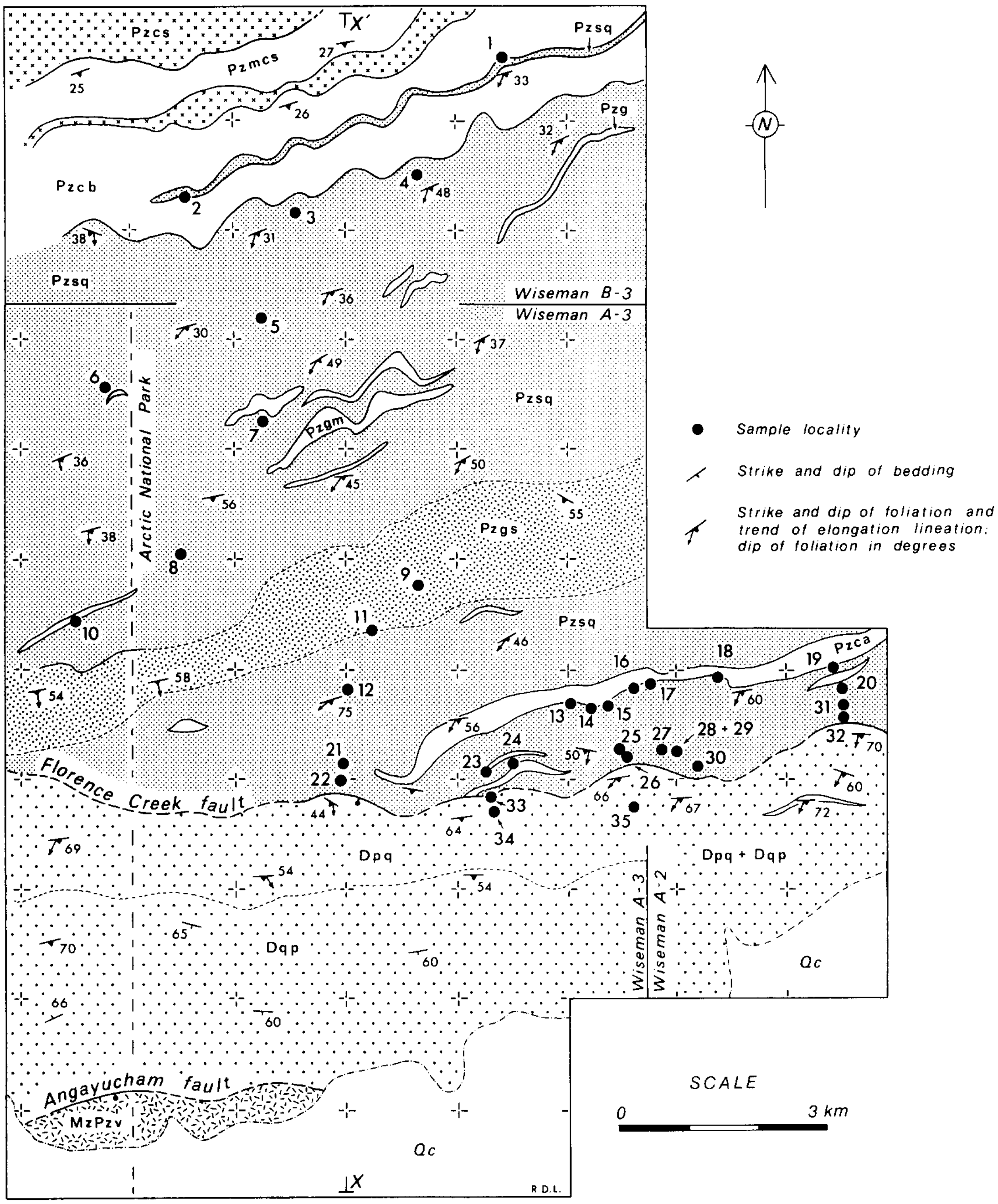

Fig. 3. Geologic map of the Florence and Fall Creeks area showing sample locations. Angayucham Terrane (Devonian–Jurassic): MzPzv = altered amygdaloidal pillow basalt. Metagreywacke–phyllite unit (? Devonian): Dqp = quartzose metasandstone with lesser slate and phyllite; Dpq = phyllite with lesser quartz-rich metasandstone. Southern Brooks Range Schist Belt (? Precambrian–Devonian): Pzsq = graphitic quartz mica schist; Pzgs = black graphitic quartz–mica schist; Pzca = schistose meta-andesite; Pzgm = massive mafic greenstone; Pzg = schistose greenstone: Pzcb = micaceous albite calc-schist, locally graphitic; Pzcs = micaceous albite calc-schist; Pzmcs = micaceous albite calc-schist interlayered with white marble. X–X' indicates line of cross-section shown in Fig. 11.

tween foliation and S_B ranges between 5° and approximately 45°, but appears to be fairly constant within individual samples. Tectonites containing such microstructures have been classified by Lister & Snoke (1984) as Type II *S–C* mylonites.

Adopting the model originally proposed by Means (1981), the sense of obliquity between foliation and preferred shape alignment (S_B) of dynamically recrystallized grains may be used as a shear-sense indicator (see also reviews by Bouchez *et al.* 1983, Simpson & Schmid 1983, Lister & Snoke 1984, Simpson 1986, Knipe & Law 1987, Jessell & Lister 1990, Hanmer & Passchier 1991).

In *XZ* thin sections viewed towards the west, a top-down-to-the-south (or sinistral) shear-sense is indicated by 20 of the 22 quartz-rich Schist Belt samples displaying an obliquity between foliation and S_B. Characteristic microstructural relationships indicating a top-down-to-the-south shear-sense are shown in Figs. 4(a) & (b). Data on both the sense and degree of obliquity between foliation and S_B within individual samples, together with sample localities, are schematically summarized in Fig. 5. Only within two samples (6 and 7) collected from the Schist Belt does the sense of obliquity between foliation and S_B indicate a top-up-to-the-north (or dextral) shear-

Table 1. Estimated distance (d) of individual samples from projected position of the Florence Creek Fault, estimated using dip-parallel cross-section drawn through the study area (Little *et al.* 1994) and measured perpendicular to the projected fault surface

Sample No.	Distance
Schist Belt	
1	7.7 km
2	6.9 km
3	6.5 km
4	6.7 km
5	4.6 km
6	4.6 km
7	4.2 km
8	3.0 km
9	2.5 km
10	1.8 km
11	1.8 km
12	1.1 km
13	1000 m
14	900 m
15	900 m
16	900 m
17	900 m
18	1000 m
19	500 m
20	250 m
21	250 m
22	200 m
23	250 m
24	250 m
25	200 m
26	<100 m
27	200 m
28	200 m
29	200 m
30	100 m
31	200 m
M–P unit	
33	<+50 m
34	+200 m
35	+400 m

sense (Fig. 5). A micrograph of the preferred grain shape alignment within a quartz-rich domain from sample 6 is presented as Fig. 4(d).

Albite porphyroblasts

Albite porphyroblasts with curving inclusion trails are present in samples 8, 10, 13, 14 and 16. Viewed towards the west, these inclusion trails define S-shaped patterns which could be interpreted as indicating a top-down-to-the-south shear sense. This interpretation assumes: (1) that the internal and external foliations associated with these porphyroblasts are contemporaneous and that either; (2) the porphyroblasts have rotated with respect to the external foliation or, (3) the porphyroblasts are overgrowing earlier S-vergent crenulations of the external foliation. However, Little *et al.* (1994) have argued that the internal and external foliations are not contemporaneous, but formed at different times and at a high angle to one another, and hence cannot be used as D_2 sense of shear indicators. A micrograph of a typical albite porphyroblast with curving inclusion trails from the Schist Belt is presented in the companion paper by Little *et al.* (1994, fig. 6c).

QUARTZ CRYSTALLOGRAPHIC FABRICS IN THE SCHIST BELT

Although some 150 oriented samples were collected from the Schist Belt, only 32 (samples 1–32) contain sufficiently quartz-rich domains for meaningful *c*-axis fabric analysis. The remaining samples contain too high a proportion of phyllosilicates (and/or other mineral phases) for fabric analysis. As previously demonstrated by Starkey & Cutforth (1978), quartz crystallographic fabrics associated with intracrystalline plasticity are generally much weaker in rocks containing a high proportion of phyllosilicate grains, because, grain boundary sliding between the quartz grains and the phyllosilicate-rich matrix disperses the developing crystallographic fabrics. In the mylonitic monomineralic quartz units located close (<250 m) to the overlying Florence Creek fault, meaningful and reproducible fabrics were detected in individual samples with a minimum of 200–300 *c*-axis measurements. At deeper structural levels in the Schist Belt, where quartz shows more evidence of recovery and is commonly only present in polymineralic aggregates, a minimum of 400–500 *c*-axis measurements were typically required for fabric analysis.

Quartz *c*-axis fabrics from the 32 Schist Belt samples are presented in Fig. 6. Location details and estimated sampling distances measured perpendicular to the projected position of the Florence Creek fault are given in Fig. 3 and Table 1, respectively. With the exception of the single girdle *c*-axis fabric displayed by sample 24, all Schist Belt samples selected for detailed petrofabric analysis are characterized by cross-girdle *c*-axis fabrics (Fig. 6). Adopting the cross-girdle fabric classification introduced by Lister (1977), the majority of these fabrics may be described as Type I cross-girdle fabrics, although fabrics closer to Type II cross-girdles are displayed by samples 5, 14, 15, 20 and 31. Some variation in both intensity distribution and skeletal outline is detected in these cross-girdle quartz fabrics.

Asymmetry in c-axis fabric intensity distribution

Asymmetry of fabric intensity distribution has been suggested by Lister & Williams (1979, p. 288) as a potential shear-sense indicator. In terms of intensity distribution, sample 24, collected at an estimated distance of 250 m beneath the Florence Creek Fault, yields the most clearly asymmetric fabric measured in the Schist Belt tectonites. This sample is characterized by an asymmetric single-girdle *c*-axis fabric containing the sample Y direction (Fig. 6). The observed fabric asymmetry indicates a top-down-to-the-south shear sense. This shear sense is also independently indicated within sample 24 by the observed sense of obliquity between foliation and S_B (Figs. 4a & b).

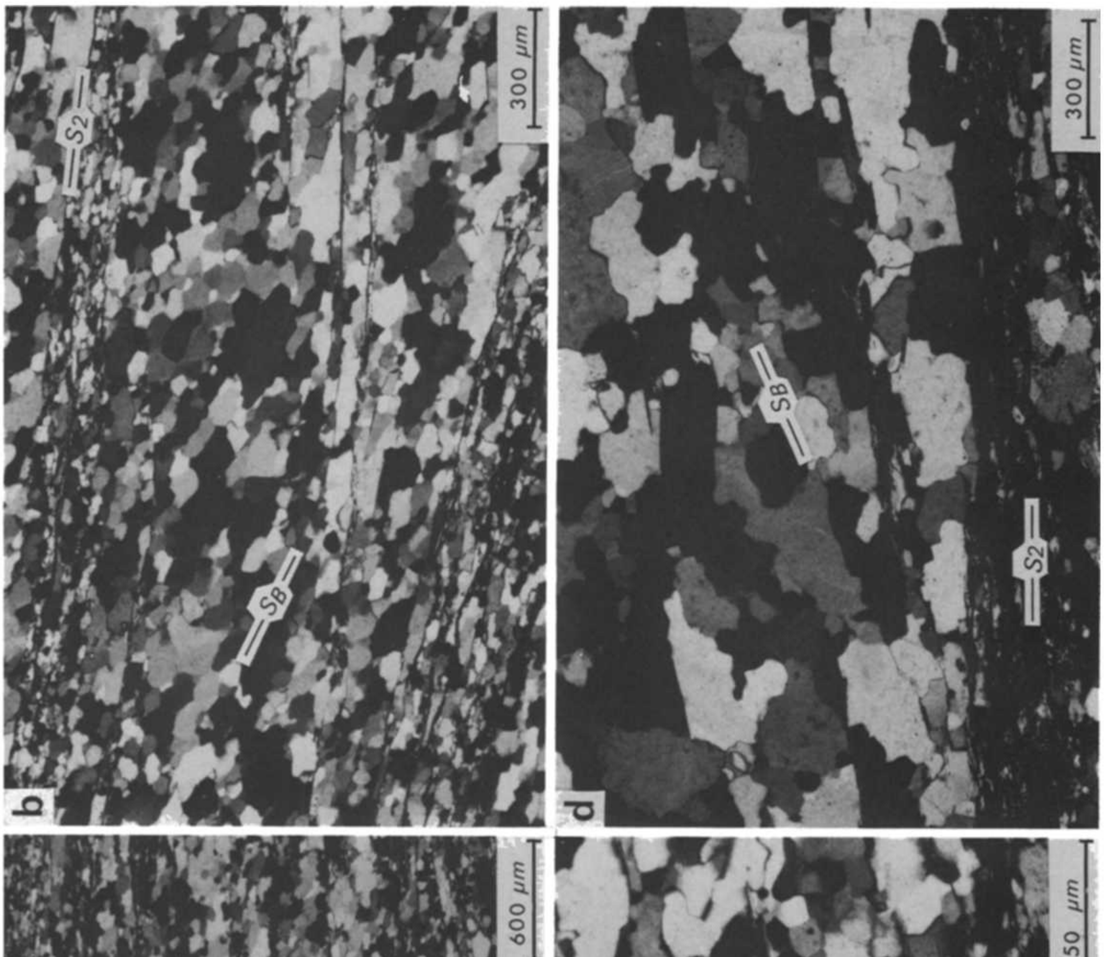

Fig. 4. Photomicrographs of elongate, dynamically recrystallized quartz grains, displaying a preferred shape alignment (S_B) oriented oblique to penetrative foliation in the Schist Belt (S_2) and MP unit (S_d). All micrographs taken from XZ sections of quartz-rich layers viewed towards the west. (a) & (b) Samples 24 from the Schist Belt—sinistral (top-down-to-the-south) shear sense indicated by sense of obliquity. (c) Quartz-vein sample 35 from the MP unit—sinistral (top-down-to-the-south) shear sense indicated. (d) Sample 6 from the Schist Belt—dextral (top-up-to-the-north) shear sense indicated. For sample localities see Fig. 3.

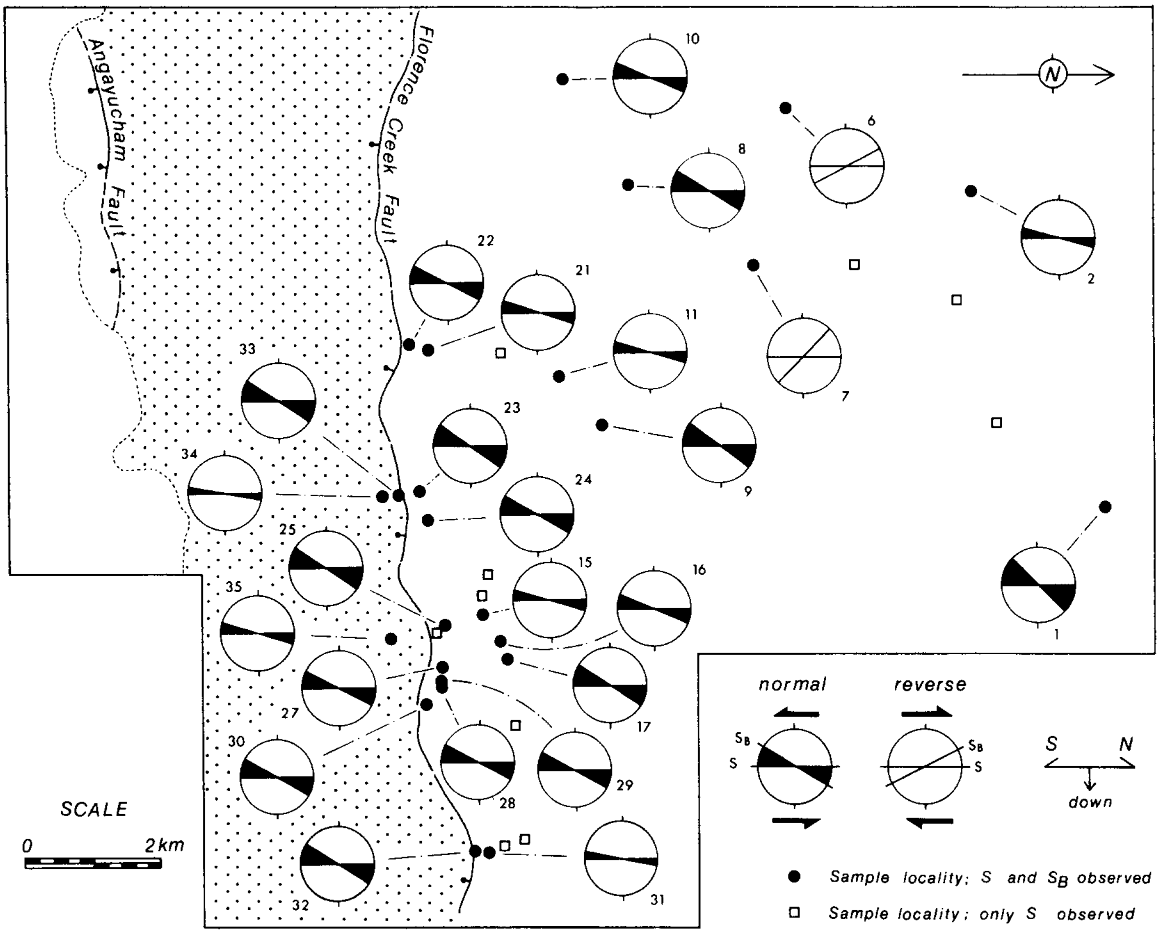

Fig. 5. Summary of observed angular relationships between penetrative foliation (S_2 in the Schist Belt, S_d in the MP unit) and preferred alignment (S_B) of elongate, dynamically recrystallized quartz grains within quartz-rich domains. Projection planes viewed towards the west and oriented perpendicular to foliation and parallel to lineation. Twenty-three of the 25 samples display an obliquity between foliation and S_B indicating a top-down-to-the-south shear sense. Stippled pattern = MP unit; unornamented area to the north of the Florence Creek Fault = Schist Belt rocks.

Less spectacular examples of asymmetry in intensity distribution consistent with a top-down-to-the-south shear sense were detected in samples 1, 8, 10, 13, 14, 15, 16, 19, 20, 22, 23, 26, 27, 28, 29, 30 and 31 (Fig. 6). In all of these samples, the obliquity between foliation and S_B (where observed) supports this inferred shear sense (Fig. 5).

A top-up-to-the-north shear sense is indicated by asymmetry of fabric intensity distribution in samples 6 and 7 (Fig. 6). This inferred shear sense is supported by the observed obliquity between foliation and S_B in both samples (Figs. 4a & b and 5).

Asymmetry in c*-axis fabric skeletal outline*

The essential topological features of a quartz *c*-axis fabric may be defined (Lister & Williams 1979) by linking up peaks and crests on the contoured diagram by a series of straight-line segments. Fabric skeletons for the Schist Belt (samples 1–32) and the overlying MP unit (samples 32–35) are shown in Fig. 7. These fabric skeletons frequently display both external and internal asymmetries; parameters used to define external and internal fabric asymmetry are illustrated in Fig. 8. Details of the external and internal fabric asymmetry elements displayed within the Schist Belt and MP unit samples are summarized in Table 2. By analogy with both experimental studies (e.g. Dell'Angelo & Tullis 1989) and simulation studies (e.g. Lister & Hobbs 1980, Etchecopar & Vasseur 1987, Jessell 1988, Jessell & Lister 1990) of quartz *c*-axis fabric development associated with non-coaxial deformation, these detected fabric asymmetries may be used as potential shear-sense indicators (e.g. Behrmann & Platt 1982, Platt & Behrmann 1986, Law 1987, 1990).

From general inspection of the skeletal outlines in Fig. 7, a top-down-to-the-south shear sense is clearly indicated in samples 1, 2, 8, 13, 16, 19, 23, 24, 25, 26, 27 and 28 from the Schist Belt. Internal fabric asymmetry may be expressed by the relative magnitudes of ω_1 and ω_2 within individual samples (Fig. 8). In each of these 12 samples, ω_2 is consistently greater than ω_1 (Table 2) indicating a top-down-to-the-south shear sense. This inferred shear sense is supported by the external fabric asymmetry parameter ψ, which varies between 60° and 75° in these samples (Table 2). External fabric asymmetry may also be expressed by the relative magnitudes of the parameters c_1 and c_2 in each sample (Fig. 8). Within 10 of 13 samples, c_1 is less than c_2 (Table 2) indicating a top-down-to-the-south shear sense. In the remaining three samples c_1 and c_2 are either equal (sample 25) or c_1 is slightly larger than c_2 (samples 2 and

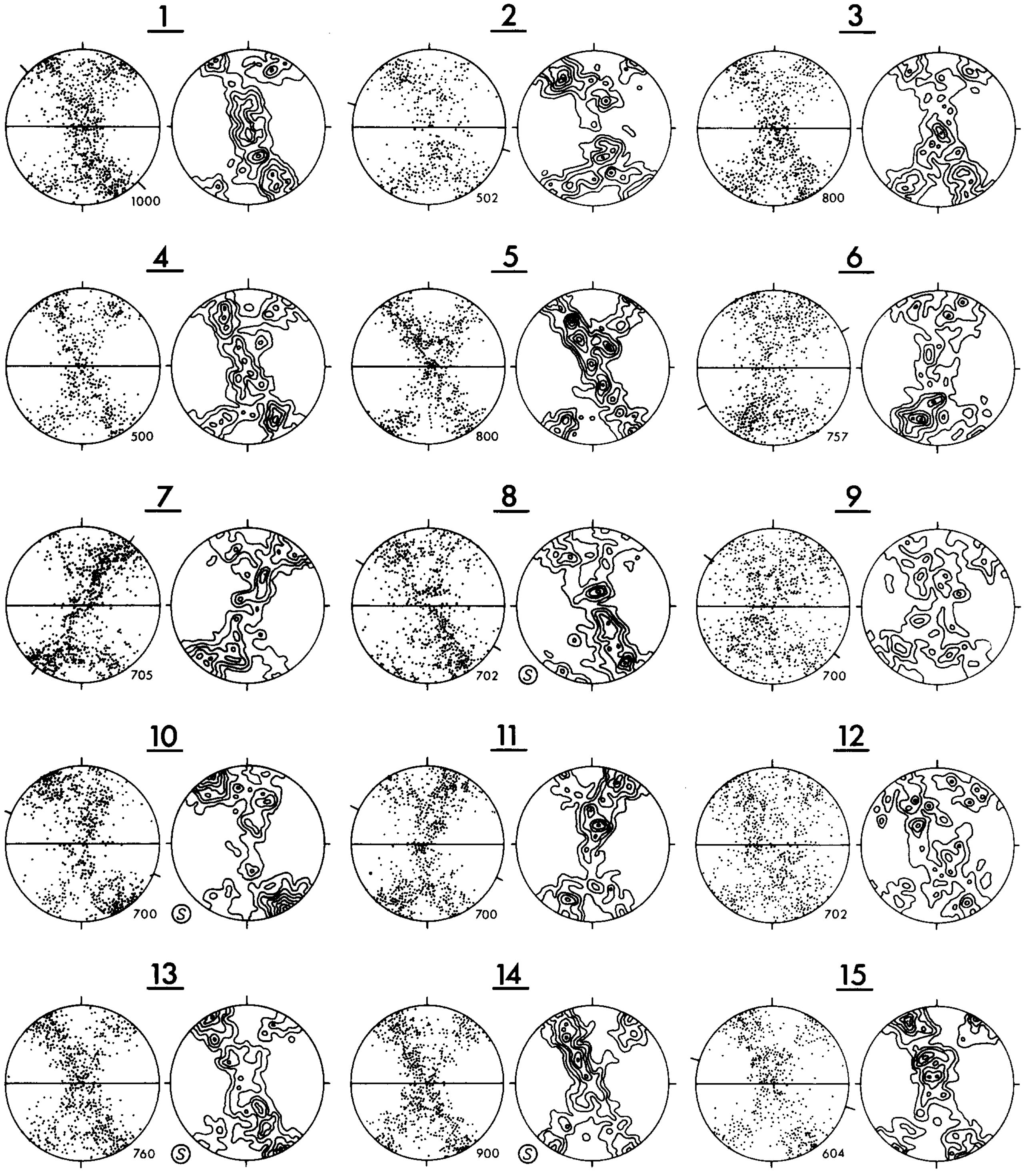

Fig. 6. Quartz *c*-axis fabrics from the Schist Belt. All lower-hemisphere, equal-area projections viewed towards the west. Contour intervals: 1, 2, 3, 4, 5, 7, 9 and 10 times uniform distribution. Orientation of foliation (S_2) and preferred alignment (S_B) of elongate dynamically recrystallized quartz grains indicated. Number of grains measured in each sample also indicated. Samples (8, 10, 13, 14 and 16) containing albite porphyroblasts with curving inclusion trails are indicated by a circled S. For sample localities see Fig. 3.

8). The top-down-to-the-south shear sense inferred from the above fabric parameters is independently confirmed in samples 1, 2, 8, 16, 19, 23, 24, 25, 27 and 28 by the observed sense of obliquity between foliation and S_B (Figs. 5, 6 and 7). No unequivocal microstructural shear sense indicators were observed in samples 13 and 26.

Less clearly defined skeletal fabric asymmetries consistent with a top-down-to-the-south shear sense were found in samples 3, 4, 15, 17, 18, 21, 29, 30, 31, 32 and 35 (Fig. 7). In each sample, this shear sense is supported by both internal fabric asymmetry (ω_2 always greater than ω_1) and the external fabric asymmetry parameter ψ which varies between 60° and 75° in these samples (Table 2). Within seven of these 11 samples, c_1 is less than c_2 (Table 2) indicating a top-down-to-the-south shear sense. In the remaining four samples c_1 and c_2 are either equal (samples 18 and 29) or c_1 is slightly larger then c_2 (samples 17 and 35). The top-down-to-the-south shear

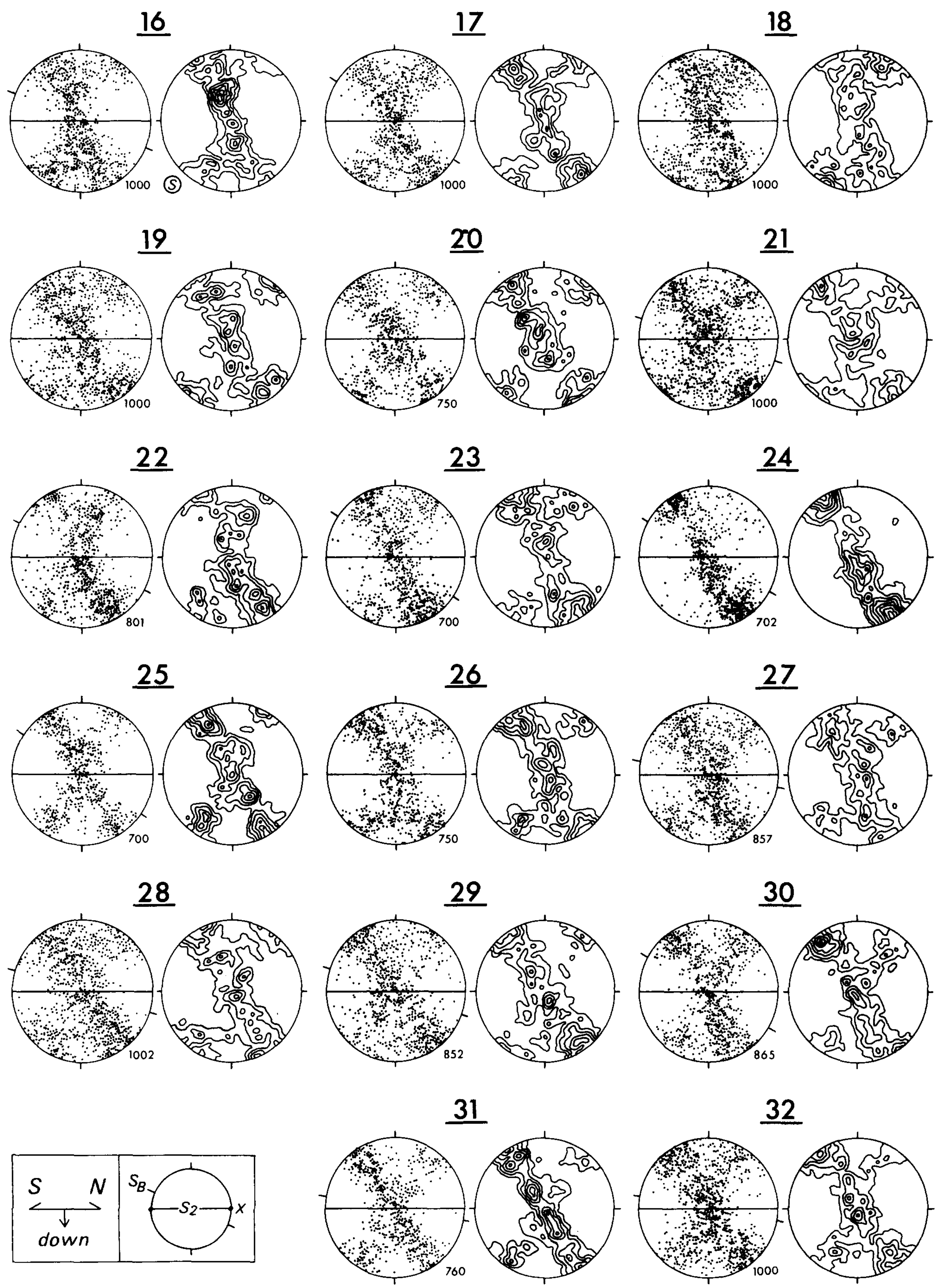

Fig. 6 (*continued*).

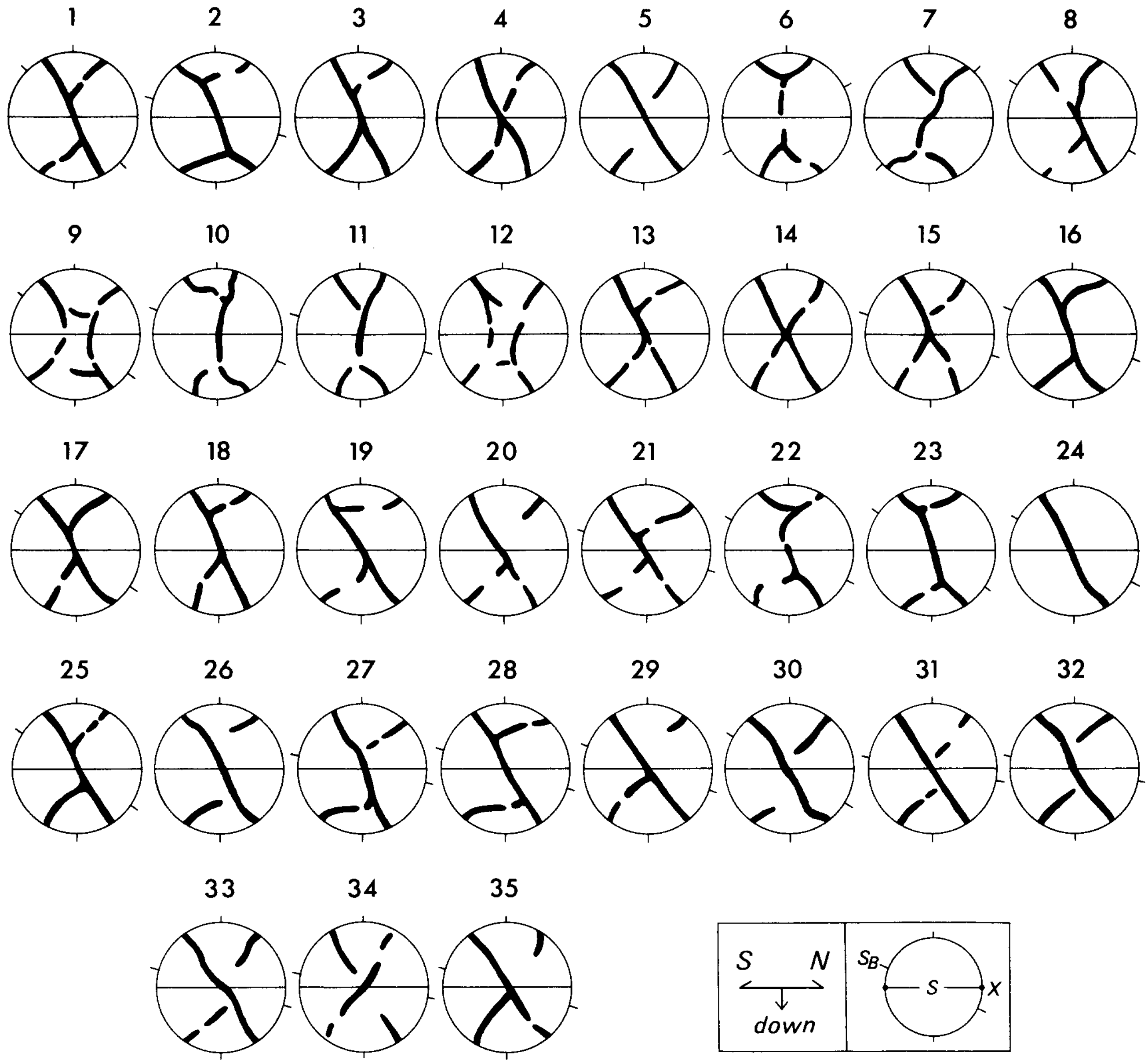

Fig. 7. Quartz *c*-axis fabric skeletons for individual samples from the Schist Belt (1–32) and the MP unit (33–35). All lower-hemisphere, equal-area projections viewed towards the west. Orientation of foliation (S_2 in the Schist Belt, S_d in the MP unit) and preferred alignment (S_B) of elongate dynamically recrystallized quartz grains indicated.

sense inferred from these less clearly defined skeletal fabrics is independently confirmed in samples 17, 21, 29, 30, 31 and 32 by the observed sense of obliquity between foliation and S_B (Figs. 5, 6 and 7). No unequivocal microstructural shear sense indicators were observed in samples 3, 4 and 18.

Skeletal fabric asymmetry indicative of top-up-to-the-north shear sense is clearly displayed in sample 7 and is confirmed by the observed sense of obliquity between foliation and S_B (Fig. 7). Less clearly defined skeletal fabric asymmetries consistent with the top-up-to-the-north shear sense were found in samples 10, 11 and 22 (Fig. 7). In all three of these samples, however, a top-down-to-the-south shear sense is indicated by the observed sense of obliquity between foliation and S_B (Fig. 7).

Symmetrical quartz c*-axis fabrics*

Quartz *c*-axis fabrics whose skeletal outlines are essentially symmetrical with respect to foliation and lineation were detected in samples 5, 6, 14 and 20 (Figs. 6 and 7). By analogy with both experimental studies (e.g. Tullis *et al.* 1973) and simulation studies (e.g. Lister & Hobbs 1980, Jessell 1988, Wenk *et al.* 1989, Wenk & Christie 1991) of quartz *c*-axis fabric development, these symmetrical fabrics could indicate a significant component of coaxial deformation. No microstructural shear-sense indicators were observed in samples 5, 14 and 20, thus supporting the proposed component of coaxial deformation in these samples. However, clear microstructural evidence for non-coaxial deformation is provided by the observed angle between foliation and S_B

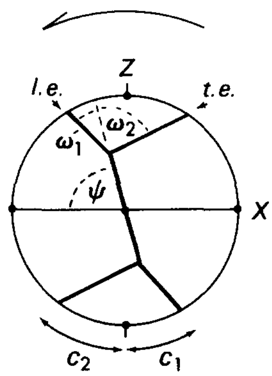

Fig. 8. Parameters used to characterize external and internal fabric asymmetry in quartz c-axis fabrics. External fabric asymmetry characterized by ψ, c_1 and c_2. Internal fabric asymmetry characterized by ω_1 and ω_2. Leading and trailing edges of the c-axis fabric skeleton denoted by l.e. and t.e., respectively. X = stretching lineation; Z = pole to foliation (S_2 in the Schist Belt, S_d in the MP unit). Fabric skeleton is based on the simulations of Lister & Hobbs (1980) for sinistral shear. In terms of Brooks Range geographic co-ordinates this diagram is viewed towards the west. Fabric asymmetry parameters are adapted from Law (1987).

in sample 6. The sense of obliquity between foliation and S_B in sample 6 indicates a top-up-to-the-north shear sense (Figs. 6 and 7).

Strain symmetry and quartz c*-axis fabrics*

Numerical modelling of quartz crystallographic fabric development (e.g. Lister & Hobbs 1980) has demonstrated a clear set of relationships between strain symmetry, fabric pattern and finite strain axes. In tectonites where no strain markers have been preserved, these fabric patterns may be used as qualitative strain symmetry indicators. For coaxially developing plane strain ($k = 1$) deformation, a symmetric cross-girdle pattern of c-axes is predicted. When dynamic recrystallization is operative during simple shear ($k = 1$) deformation, similar symmetric cross-girdle fabrics may develop at low shear strains and progressively change through asymmetric cross-girdle fabrics to single-girdle fabrics with increasing shear strain (e.g. Etchecopar & Vasseur 1987, Jessell & Lister 1990). In contrast, while coaxially developing flattening strains ($k = 0$) are characterized

Table 2. Details of quartz c-axis external and internal fabric asymmetry within samples 1–35. For explanation of asymmetry parameters used see Fig. 8. All measurements for individual samples made on projection planes viewed towards the west. Thus, for example, a ψ value of less than 90° would indicate a top-down-to-the-south (sinistral) shear sense, while a ψ value greater than 90° would indicate a top-up-to-the-north shear sense

Sample No.	ψ	C_1	C_2	ω_1	ω_2	d	No. of c-axes
			Quartz-rich layers in the Schist Belt				
1	71°	26°	31°	12°	52°	7.7 km	1000
2	73°	34°	32°	37°	87°	6.9 km	502
3	71°	23°	29°	13°	63°	6.5 km	800
4	62°	23°	32°	—	—	6.7 km	500
5	65°	32°	31°	8°	78°	4.6 km	800
6	90°	30°	26°	50°	50°	4.6 km	757
7	115°	20°	38°	68°	32°	4.2 km	705
8	62°	30°	27°	10°	45°	3.0 km	702
9	—	34°	45°	—	—	2.5 km	700
10	95°	30°	18°	—	—	1.8 km	700
11	102°	23°	24°	50°	15°	1.8 km	700
12	—	28°	38°	—	—	1.1 km	702
13	64°	26°	34°	−12°	78°	1000 m	760
14	62°	28°	34°	0°	60°	900 m	900
15	64°	28°	33°	20°	75°	900 m	604
16	71°	30°	36°	18°	68°	900 m	1000
17	70°	34°	30°	12°	60°	900 m	1000
18	75°	26°	26°	20°	55°	1000 m	1000
19	68°	33°	36°	0°	120°	500 m	1000
20	65°	30°	36°	0°	90°	250 m	750
21	70°	32°	37°	0°	90°	250 m	1000
22	73°	28°	30°	—	—	200 m	801
23	72°	30°	25°	30°	85°	250 m	700
24	70°	30°	—	15°	—	250 m	702
25	65°	30°	30°	0°	85°	200 m	700
26	70°	35°	36°	31°	90°	<100 m	750
27	75°	28°	42°	22°	68°	200 m	857
28	65°	30°	42°	19°	90°	200 m	1002
29	58°	34°	34°	0°	90°	200 m	852
30	67°	36°	37°	28°	76°	100 m	865
31	60°	32°	34°	0°	75°	200 m	760
32	73°	3°	36°	28°	64°	<100 m	1000
			Quartz veins in the metagreywacke–phyllite unit				
33	60°	32°	36°	—	—	<+50 m	850
34	—	30°	30°	—	—	+200 m	910
35	60°	38°	32°	33°	75°	+400 m	750

by small-circle girdle distribution of *c*-axes centered about the pole (Z) to foliation, coaxial extensional strains ($k = \infty$) should be characterized by a small-circle distribution centered about the stretching lineation (X). These relationships are supported by both experimental studies (e.g. Green *et al.* 1970, Tullis *et al.* 1973, Tullis 1977, Dell'Angelo & Tullis 1989) and analysis of naturally deformed quartzites (see reviews by Price 1985, Schmid & Casey 1986, Law 1990).

With only three exceptions, all the samples selected for detailed fabric analysis within the Schist Belt are characterized by cross-girdle quartz *c*-axis fabrics. By analogy with the above numerical and experimental studies, these cross-girdle fabrics (together with the single girdle fabric displayed by sample 24) are inferred to indicate approximately plane strain ($k = 1$) deformation conditions. Also by analogy with the above studies, these crystal fabrics confirm that the down-dip mineral elongation (X) observed in outcrop (Fig. 3) indicates the local maximum principal finite extension direction.

Samples 9 and 12 from the Schist Belt are characterized by quartz *c*-axis fabrics which appear to be transitional between a cross-girdle fabric and a small-circle girdle fabric of large opening angle centered about a pole oriented close to the lineation (Figs. 6 and 7). By analogy with the above studies, these fabrics may indicate deformation within the constrictional ($k > 1$) field.

SHEAR-SENSE INDICATORS IN THE METAGREYWACKE–PHYLLITE BELT

Microstructures

Rocks in the MP unit are cut by a single well-developed foliation that is axial planar to mesoscopic folds of bedding and dips moderately towards the south (Fig. 3). This foliation is referred to as S_d by Little *et al.* (1994).

In pelitic rocks, S_d is a domainal cleavage defined by alignment of micaceous films and trails of graphitic dust concentrated along pressure solution seams. In metagreywacke, S_d is a rough cleavage defined by flattened detrital quartz grains, anastomosing films of white mica and chlorite, and fibrous beards of white mica and quartz. The importance of diffusive mass transfer in these tectonites is indicated by the truncation of spindle-shaped quartz grains against discrete cleavage seams of micaceous and graphitic residue. Crystal-plastic deformation of quartz, as indicated by undulatory extinction and subgrain development in detrital grains, was a subsidiary deformation mechanism in the pelites and metagreywackes, but the dominant mechanism in the foliation-parallel monomineralic quartz veins which cut these lithologies. The most strongly deformed metagreywacke occurs adjacent to the Florence Creek Fault (Fig. 3). These flaggy mylonitic schists contain a down-dip mineral elongation lineation defined by ribbon shaped, original detrital quartz grains.

Of the 50 oriented samples collected from the MP unit, only three (samples 33–35) contain sufficiently quartz-rich domains for meaningful *c*-axis fabric analysis; the remaining samples contain too high a proportion of phyllosilicates (cf. Starkey & Cutforth 1978). All three samples selected for detailed fabric analysis were taken from metagreywacke exposures located close to the Florence Creek Fault (Figs. 3 and 8).

The quartz-rich domains in the selected samples have been derived from original quartz vein material. In XZ thin sections, the veins define 1–2 mm wide ribbons oriented parallel to foliation in the surrounding matrix. The veins are composed of elongate, dynamically recrystallized quartz grains displaying a preferred shape alignment (S_B) which is oblique to foliation (Fig. 4c). In all three samples (33–35) the sense of obliquity between foliation and S_B indicates a top-down-to-the-south shear sense (Figs. 5 and 9). No unequivocal microstructural shear sense indicators were observed in the surrounding phyllosilicate-rich matrix.

Quartz crystallographic fabrics

Optically measured *c*-axis fabrics from dynamically recrystallized quartz veins within the three metagreywacke samples are presented in Fig. 9. All three samples yield diffuse cross-girdle fabrics which are weakly asymmetric with respect to foliation and lineation in terms of skeletal outline and density distribution (Figs. 5, 7 and 8). The fabric asymmetry is consistent with the top-down-to-the-south shear sense indicated by the obliquity between foliation and S_B in these quartz veins (Figs. 4c and 5). The cross-girdle fabric pattern indicates that all three samples are approximate plane strain

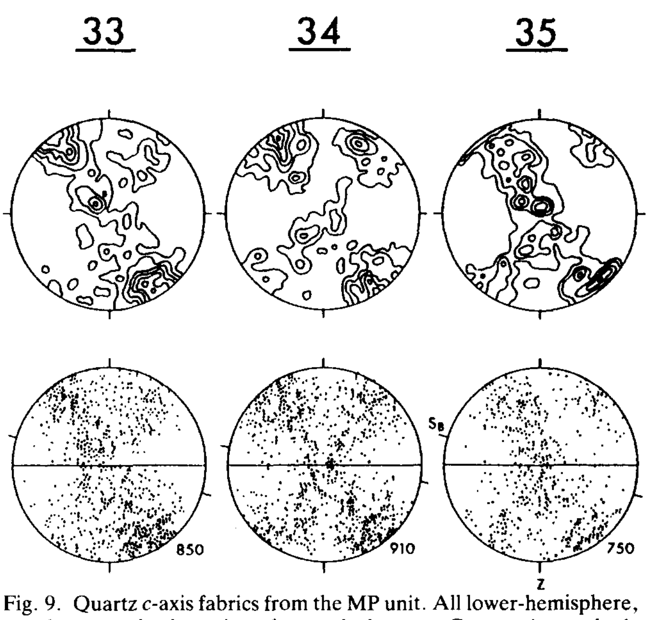

Fig. 9. Quartz *c*-axis fabrics from the MP unit. All lower-hemisphere, equal-area projections viewed towards the west. Contour intervals: 1, 2, 3, 4, 5, 7, 9 and 10 times uniform distribution. Z = pole to foliation (S_d), S_B = preferred alignment of elongate dynamically recrystallized quartz grains. Number of grains measured in each sample also indicated. For sample localities see Fig. 3.

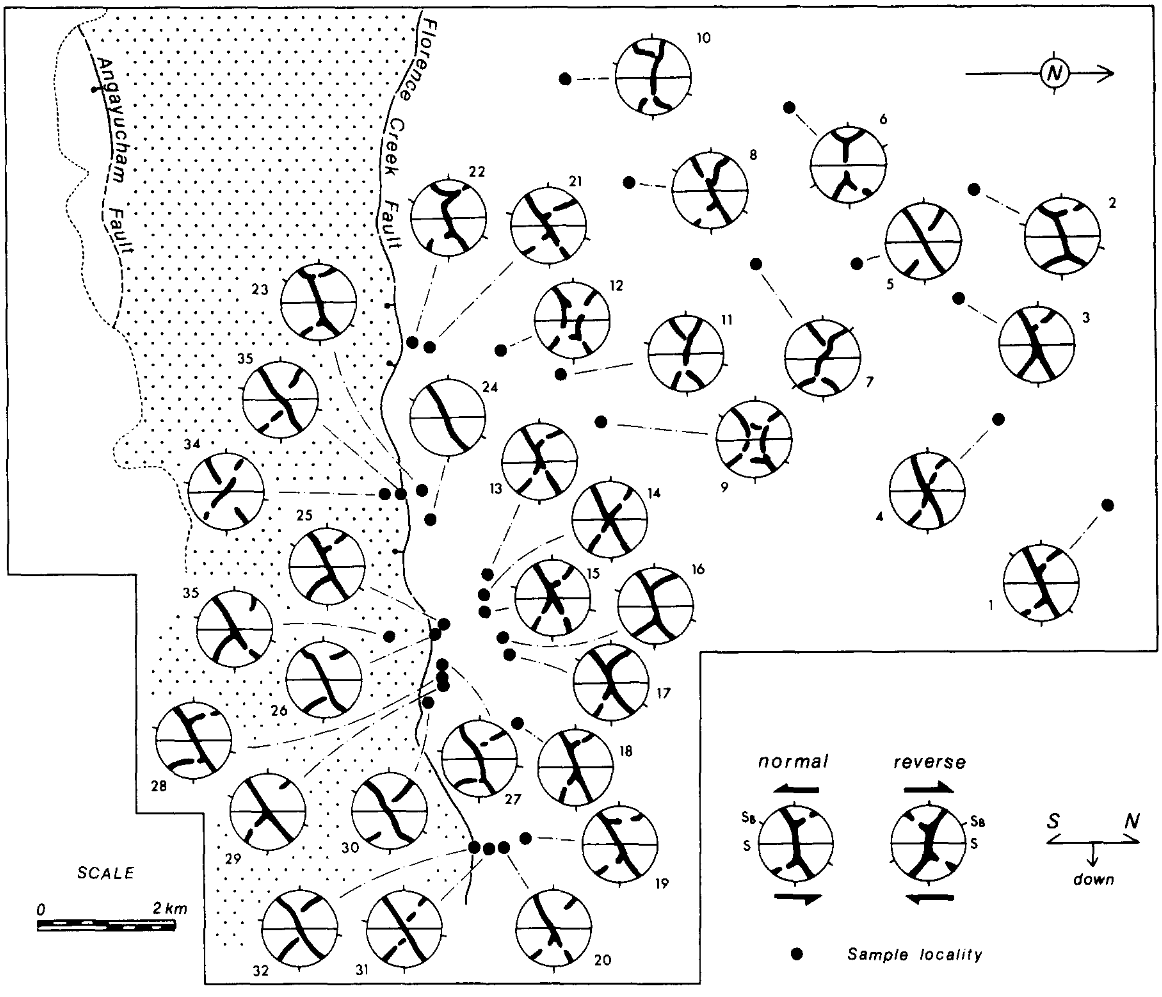

Fig. 10. Summary diagram of quartz *c*-axis fabric skeletons within the study area. Schist Belt: samples 1–32, MP unit: samples 33–35. All lower-hemisphere, equal-area projections viewed towards the west. Orientation of foliation (S_2 in the Schist Belt, S_d in the MP unit) and preferred alignment (S_B) of elongate dynamically recrystallized quartz grains indicated. Stippled pattern = MP unit; unornamented area to the north of the Florence Creek Fault = Schist Belt rocks.

tectonites, and that the down-dip mineral lineation is a true stretching lineation.

DISCUSSION

Kinematic indicators

Tectonites of the Florence and Fall Creeks study area display a strongly developed S-dipping greenschist facies foliation and associated down-dip mineral stretching lineation. Two shear-sense indicators were particularly useful in distinguishing between crystal-plastic deformation associated with top-down-to-the-south and top-up-to-the-north shear senses in quartz-rich lithologies from both the Schist Belt and the overlying MP unit. These shear-sense indicators are: (1) sense of obliquity between foliation and preferred shape alignment (S_B) of elongate dynamically recrystallized quartz grains; and (2) asymmetry of quartz *c*-axis fabric with respect to foliation and lineation.

The geographic distribution of sampling localities in which an obliquity between foliation and S_B is detected is summarized in Fig. 5. A dominant top-down-to-the-south shear sense is indicated by the observed sense of obliquity between foliation and S_B. This inferred shear sense is strongly supported by the generally observed sense of asymmetry of the quartz *c*-axis fabrics. The skeletal outlines of these fabrics, together with sample localities, are schematically summarized in Fig. 10. These microstructures and crystal fabrics are clearly related to formation of both the single foliation (S_d) in the MP unit and the dominant foliation (S_2) recognized by Little *et al.* (1994) in the southern part of the Schist Belt.

We emphasize that all analyzed samples were collected from outcrops displaying a single, homogeneously developed, penetrative foliation equivalent to S_d–S_2 of Little *et al.* (1994). No reported samples were collected from discrete shear zones, such as the late stage shear bands described by Little *et al.* (1994, fig. 5c) or from rocks where S_1 is locally preserved. The kinematic interpretation of an individual sample is therefore regarded as being valid up to at least the scale of the outcrop from which it was taken. A simplified down-dip cross-section through the area, together with quartz *c*-axis fabrics considered to be representative of different

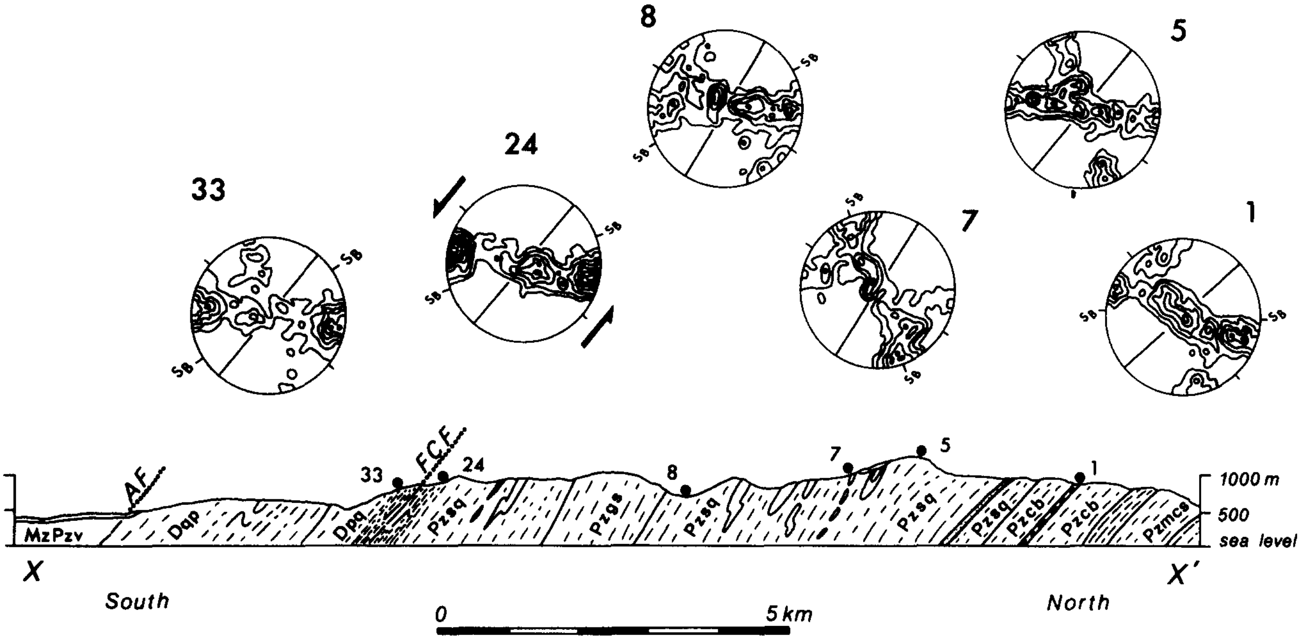

Fig. 11. N–S cross-section through the study area, line of section shown as X–X′ in Fig. 3. A.F = Angayucham Fault; F.C.F. = Florence Creek Fault. Representative quartz *c*-axis fabrics from six samples are shown. All lower-hemisphere, equal-area projections viewed towards the west. Orientation of foliation (solid line) and preferred alignment (S_B) of elongate dynamically recrystallized quartz grains indicated. In these samples, a top-up-to-the-north shear sense is only indicated by fabric asymmetry and obliquity between foliation and S_B in sample 7. For explanation of lithology symbols and fabric contour intervals, see Figs. 3 and 6, respectively.

depths beneath the Florence Creek Fault, is shown in Fig. 11.

Within the Florence and Fall Creeks study area, only extremely limited microstructural and crystal fabric evidence has been found for penetrative deformation associated with a top-up-to-the-north shear sense. At least in the quartz-rich samples selected for detailed fabric analysis, a top-up-to-the-north shear sense is only indicated by sense of *c*-axis fabric asymmetry and obliquity between foliation and S_B in samples 6 and 7 (Figs. 6 and 7). These Schist Belt samples were collected at approximately 4.6 km (sample 6) and 4.2 km (sample 7) beneath the projected position of the Florence Creek Fault (Figs. 5 and 10).

Microstructural and crystal fabric evidence for a significant component of coaxial deformation within quartz-rich units from the Schist Belt has only been recorded in samples 5, 14 and 20 (Fig. 7). In contrast, microstructural evidence for coaxial deformation is more common in the pelitic *L–S* tectonites and many of the additional 165 quartz-poor samples from the Schist Belt and MP unit lack convincing shear-sense indicators (Little *et al.* 1994). Symmetric pressure shadows in some of these samples indicate approximate coaxial deformation histories involving bulk shortening perpendicular to foliation and extension parallel to lineation. These observations suggest that lithology-controlled strain path partitioning may have operated in the Schist Belt rocks.

In many well-documented mylonite zones, both strain magnitude and degree of crystal fabric asymmetry increase towards associated fault contacts. Examples include the Moine thrust of NW Scotland (Law *et al.* 1986, Law 1987), the Betic Cordilleras of SE Spain (Platt & Behrmann 1986) and the Snake Range detachment of Nevada, U.S.A. (Lee *et al.* 1987). For the quartz-rich units of the Brooks Range Schist Belt, although it is true that mylonitic textures are only found at less than 250 m from the Florence Creek Fault, and that the most asymmetric fabrics are generally recorded close to the fault, no convincing progressive increase in degree of fabric asymmetry, traced towards the fault, has been detected (Figs. 8 and 10). The possible importance of progressive strain path partitioning with distance beneath the Florence Creek fault therefore remains unclear.

Tectonic interpretation of kinematic indicators

In the companion paper to this microstructural and crystal fabric analysis, Little *et al.* (1994) have argued that the S-dipping penetrative foliation (S_2 in the Schist Belt, S_d in the overlying MP unit) and down-dip stretching lineation recognized in the Florence and Fall Creeks area, developed during a period of mid-Cretaceous crustal extension associated with top-down-to-the-south shearing. This extensional interpretation is compatible with the fact that along the S-dipping, foliation-parallel Florence Creek Fault, very low grade rocks (MP unit) in the hangingwall rest on completely recrystallized polydeformed rocks of the Schist Belt that retain evidence for an early (D_1) high-*P*–low-*T* event. Most of the MP unit contains a rough or slaty cleavage formed chiefly by pressure solution and represents a higher structural level of exposure than the underlying Schist Belt. Little *et al.* (1994) infer that these two packages of rocks, metamorphosed at different crustal levels during the M1 event, were juxtaposed prior to (or during) development of the

S_d–S_2 foliation. Within both the MP unit and the Schist Belt, the most intensely deformed rocks, showing the least evidence for recovery processes, occur within 300 m of the Florence Creek Fault.

Both the oblique quartz grain shape alignments and the asymmetric quartz *c*-axis fabrics which indicate a top-down-to-the-south shear sense in the MP unit and Schist Belt tectonites (Figs. 5 and 10) are compatible with this extensional model. It should be emphasized that the microstructural and crystal fabric evidence for extension in the Florence and Fall Creeks area is not limited to a relatively narrow zone of penetrative deformation. Within the Schist Belt rocks, evidence for top-down-to-the-south shear has been found in samples collected at estimated distances ranging from less than 100 m beneath the projected position of the Florence Creek Fault, to approximately 7.7 km beneath the fault (Figs. 8 and 11). In the overlying MP unit, evidence for extensional deformation has been found in quartz veins located at distances of between 50 and 400 m above the fault.

These observations indicate that the Florence and Fall Creeks study area is situated over a large scale (at least 8.1 km thick) zone of extensional shear dipping towards the south. Within this zone (Fig. 11), only two of the 35 samples analyzed contained microstructures and crystal fabrics indicating a top-up-to-the-north shear sense (samples 6 and 7 in Figs. 5 and 10). The two Schist Belt samples exhibiting the opposite shear sense may represent zones of conjugate shear or flow within the broader zone of extensional (top-down-to-the-south) deformation (Little *et al.* 1994). Alternatively, they could represent regions of low D_2 strain within which earlier D_1 thrust-related fabrics have locally been preserved.

The concept of a regionally important phase of mid-Cretaceous extension-related penetrative deformation in the Brooks Range is highly controversial (see recent discussion by Miller & Hudson 1993 and Till *et al.* 1993). Models for extensional deformation in other mountain belts have been similarly controversial, and numerous examples have been documented where locally important *apparent* extensional geometries may, in fact, be related to thrusting. For example, Wheeler (1991) has demonstrated that in the European Alps normal-sense metamorphic breaks, such as that between the greenschist-facies Combin zone, and the structurally underlying Zermatt-Saas eclogite-facies zone (Platt 1986) could, in principal, be accounted for by either out-of-sequence thrusting or backthrusting within an orogenic wedge. In the case of the south-central Brooks Range, the dominant top-down-to-the-south shear sense associated with foliation development is incompatible with out-of-sequence N-directed overthrusting but could, theoretically, be related to S-directed backthrusting. However, in order to be compatible with the structural relationships mapped by previous workers (e.g. Dillon *et al.* 1981, 1986, 1987, Little *et al.* 1994) such an originally S-directed, N-dipping backthrust would subsequently either have to be: (1) tilted through the vertical (assuming no previous structural inversion of lithotectonic units) in order to place the MP unit on top of the Schist Belt; or (2) tilted through the horizontal (assuming previous structural inversion). We regard these backthrust interpretations as being unlikely because low-grade rocks structurally overlie high-grade rocks along the entire length (>500 km) of the southern Brooks Range. Furthermore, the Cretaceous clastic strata overlying these tectonites are not overturned.

Strain estimates

Movement on the zone of extensional shear in the Florence and Fall Creeks area has been correlated by Little *et al.* (1994) with development of the Yukon–Koyukuk basin to the south (Fig. 1). The basin contains a 5–8 km thick section of early Cretaceous (Berriasian–Aptian) volcanics overlain by terrigenous sedimentary rocks (Albian–Cenomanian) (Nilsen 1989, Patton & Box 1989). A very crude estimate of displacement across the zone may also be made by considering the strain required to produce the observed top-down-to-the-south quartz *c*-axis fabrics. Little *et al.* (1994) have argued that these extension-related fabrics have been produced by overprinting of earlier thrust-related fabrics. Fabric simulation studies by Lister and co-workers indicate that in quartzites 40% shortening is sufficient to result in gross changes to a previously existing fabric (Hobbs 1985, p. 477). Assuming simple shear deformation, this 40% shortening corresponds (Ramsay 1967, p. 85) to a shear strain, γ, of 1.07. A displacement of 8.6 km is indicated by assuming a homogeneous strain across an 8.0 km thick zone of simple shear.

Although the fabric analyses indicate that: (1) deformation within the inferred shear zone approximates plane strain; and (2) the component of non-coaxial (simple shear) deformation is dominant over any coaxial (pure shear) component (at least in the quartz-rich samples analyzed), the absolute magnitudes of these components remain unknown. The observed parallelism between foliation and the projected tectonic boundary between the Schist Belt and the overlying MP unit may, for example, indicate a significant component of pure shear deformation. Such a pure shear component would necessitate reducing the above displacement estimate which was made by assuming simple shear alone.

Crude shear strain estimates may also be obtained by considering the pattern of quartz *c*-axis preferred orientation. For computer-simulated simple shear deformation, Jessell & Lister (1990) have demonstrated a progressive transition, with increasing shear strain, from cross-girdle to single-girdle quartz *c*-axis fabrics under conditions where both crystal slip and dynamic recrystallization are important. The transition from cross-girdle to single-girdle fabrics in these simulations occurs in a shear strain, γ, range of between 0.7 and 1.5. The Schist Belt and MP unit are characterized by cross-girdle fabrics; a single-girdle fabric has only been recorded in sample 24 located at 250 m beneath the Florence Creek fault (Fig. 11). By correlation with the simulation work of Jessell & Lister (1990) these cross-girdle fabrics also indicate low shear strains associated with fabric and foliation development.

The presence of N-vergent folds in the southern part of the Florence and Fall Creek area may also be used to obtain crude shear estimates assuming that they formed during top-down-to-the-south movement. Little *et al.* (1994) have demonstrated that these apparently anomalous N-verging D_2 folds could either be explained by: (1) a strong component of pure shear deformation being obliquely imprinted on dipping layering; or (2) fold development within a S-dipping, top-down-to-the-south, shear zone when the initial layering dipped more steeply to the south than the shear zone boundaries. A geometrically similar situation to the second possibility has been modelled numerically by Ramsay *et al.* (1983) assuming homogenous simple shear. By analogy with the results presented by Ramsay *et al.* (1983, fig. 4) a minimum shear strain, γ, of between 6.0 and 8.0 is required to produce a series of N-vergent folds in a top-down-to-the-south shear zone. This minimum shear strain could be reduced considerably if there was a significant component of pure shear deformation, which we believe is likely.

Larger shear strains may locally be indicated in the Schist Belt by sheath folds whose axial planes are parallel to S_2 (Little *et al.* 1994); experimental studies under homogeneous simple shear conditions (e.g. Cobbold & Quinquis 1980) indicate that shear strains, γ, of greater than 10 are required for sheath fold development when the shearing plane is oriented parallel to the sheet dip of the layering. Large-magnitude strains are also indicated by the apparent *ca* 70° rotation of $L_{1\times2}$ intersection lineations which, traced from north to south in the Florence and Fall Creeks area, change in orientation from gentle west or east plunges to nearly down-dip trends (Little *et al.* 1994, figs. 3 and 7).

Correlation with previously published along-strike studies

How far this large-scale zone of extensional (or top-down-to-the-south) shear can be traced along strike remains unclear. In the Cosmos Hills, located 200 km along strike to the west of the Florence and Fall Creek study area (Fig. 1b), Box (1987) and Christiansen (1989) described extensional faults of post-Early Cretaceous age where a strong foliation overprints inferred fault contacts between Schist Belt rocks, the MP unit and the Angayucham terrane. The foliation is also present as a weak fabric in overlying fault-bounded Cretaceous sediments of the Yukon–Koyukuk basin. Thus, if contacts between units along the southern flank of the range are normal faults, ductile deformation of inferred extensional origin may be synchronous with and/or post-date motion on these faults (Little *et al.* 1994). Christiansen (1989) described asymmetrical quartz *c*-axis fabrics indicating a top-down-to-the-south shear sense within the Schist Belt rocks of the Cosmos Hills. This inferred shear sense is also independently indicated by asymmetric pressure shadows on pre-tectonic porphyroblasts within these tectonites.

In contrast, quartz fabrics indicating a top-up-to-the-north shear sense have been documented by Gottschalk (1987, 1990) in Schist Belt rocks immediately east of the Trans-Alaska pipeline and to the north of Coldfoot (Fig. 1b). Gottschalk (1990) recognizes three deformation events in these tectonites, which are located some 30 km along strike to the east of the Florence and Fall Creeks study area. The dominant foliation, which is referred to as S_{1b} by Gottschalk (1990), is flexed into a broad asymmetric antiform known as the Wiseman arch. This foliation has been correlated by Little *et al.* (1994) with the S_2 foliation recognized in the Schist Belt rocks of the Florence and Fall Creeks study area. Although D_{1b} strains in the Wiseman area are locally heterogeneous, they do appear to increase to the south in the higher levels of the section (R. Gottschalk personal communication 1992) in a similar manner to that recorded for D_2 in the Florence and Fall Creeks area. In contrast to our study area, no macroscopically obvious stretching lineation is observed on the S_{1b} foliation surfaces in the Wiseman area. However, a N–S-trending, down-dip stretching direction may be inferred from the pole-free areas of the *c*-axis fabrics in these tectonites (R. Gottschalk personal communication 1992).

Twelve quartz *c*-axis fabrics have been reported by Gottschalk (1990, fig. 2) from the Wiseman arch. Although of a generally diffuse nature, nine of these fabrics display a fairly convincing asymmetry with respect to foliation (S_{1b}) and lineation (L_{1b}). In only one of these fabrics is a top-down-to-the-south shear sense indicated by fabric asymmetry, the remaining eight fabrics indicating a top-up-to-the-north shear sense. A further two more weakly defined, unpublished fabrics also indicate a top-down-to-the-south shear sense (R. Gottschalk personal communication 1992). All three top-down-to-the-south fabrics are from the higher levels of the section to the south where D_{1b} strains are higher.

Clearly, if S_2 in the Florence and Fall Creeks study area and S_{1b} of Gottschalk (1990) in the Wiseman arch are coeval then there is a major conflict in the kinematic interpretation of deformation associated with the formation of these structures in the two areas. One possible solution to this apparent conflict is that S_{1b} in the Wiseman area is related to the earlier D_1 thrusting event recognized in the Florence and Fall Creeks area, and has been overprinted by a weaker extensional deformation (characterized by extensional shear bands). Gottschalk (1990, p. 463) noted that within the Wiseman area, folds with 'S-vergent asymmetry' indicate that the Schist Belt was affected by a relatively late-stage event involving top-down-to-the-south shear. This interpretation could be supported by the 'geometry and orientation of ductile extensional shear bands' in the Wiseman area of the Schist Belt (Gottschalk 1990, p. 465).

An alternative solution is that S_{1b} in the Wiseman area is extensional in origin, and extension-related strain may be greater in the Florence and Fall Creeks area than in the Wiseman area. This would produce: (1) a predominance of top-down-to-the-south shear senses in the Florence and Fall Creeks area; (2) a zone of mixed shear senses in the southern part of the Wiseman area; and (3) a predominance of relict top-up-to-the-north shear senses elsewhere in the Schist Belt where extensional shear strains are relatively low (R. Gottschalk personal communication 1992). Resolution of this problem of along-strike shear-sense correlation can only be achieved by new studies in the intervening ground.

Kinematic indicators and shortening vs extension-related fabrics: comparison with examples from Europe and the Himalayas

Evidence for extensional deformation on the southern flank of the Brooks Range has been documented using microstructural and petrofabric data (reported in this paper) in combination with petrologic, structural and radiometric age analyses (see companion paper by Little *et al.* 1994). As outlined in the Introduction to this paper, single pieces of evidence for extensional deformation in contractional orogens are rarely unequivocal, but when several complementary lines of evidence come together (as we have attempted to demonstrate for the Brooks Range) then the case becomes more compelling. If we are correct in our extensional interpretation of deformation features preserved in the Brooks Range, then it is clearly of interest to know how common such features are in other compressional orogens. Below we briefly review the results of several previously published studies in Europe and the Himalayas which have used similar analytical techniques to those employed in our study.

Particularly spectacular examples of the use of kinematic indicators in distinguishing between shortening and extension-related fabrics have been described from the Sognefjord–Nordfjord and Roragen areas of western Norway where regional extension is thought to have been generated due to the collapse of overthickened crust at the end of the Caledonian continent–continent collision (Norton 1986). Northwest-dipping mylonite zones in these areas have traditionally been related to Caledonian SE-directed thrusting. However, kinematic analyses of these zones using shear bands (Séranne & Séguret 1987), asymmetric quartz crystal fabrics and oblique quartz grain shape alignments (Norton 1987, Norton *et al.* 1987, Chauvet & Brunel 1988, Brunel & Chauvet 1993) indicate a top-down-to-the-northwest movement sense. These thick (>100 m) mylonite zones cross-cut the underlying Caledonian (pre-Devonian) basement structures, and define the margins of overlying Devonian age half-graben sedimentary basins. The mylonites have been interpreted by Norton (1987) as marking a regionally important extensional detachment which displaced a weakly metamorphosed upper plate carrying syn-extensional clastic sediments. The detachment structure consists of a *ca* 10 m thick shear zone (partly cataclastic) passing down into a thick sequence of mylonites derived from cover sedimentary rocks in the upper part, and basement tectonites in the lower part, and varying from greenschist- to mid-amphibolite-facies from top to bottom (Norton 1987). This Norwegian example clearly bears some geometric similarities to the model proposed by Miller & Hudson (1991) for extensional deformation in the Brooks Range and development of the Yukon–Koyukuk basin to the south (see also Little *et al.* 1993, fig. 9c).

Shear-sense indicators such as asymmetric crystal fabrics have also been used to distinguish between mylonite zones associated with normal and reverse senses of motion in the Austrian Alps. Motion on the normal-sense mylonite zones has been related to both formation of sedimentary basins (e.g. Krohe 1987) and the exhumation of high pressure metamorphic mineral assemblages (e.g. Behrmann & Ratschbacher 1989) during late Cretaceous crustal extension. Similarly in the western Alps, Wheeler & Butler (1993) have used kinematic indicators such as shear bands to distinguish between foreland and hinterland directed fault zones and have argued that movement on the hinterland directed faults may be, at least in part, of extensional origin. Other examples of the application of shear-sense indicators for distinguishing between shortening and extension-related fabrics have been described by Powell & Glendinning (1990) from the Caledonides of northern Scotland, and by Malavieille *et al.* (1990) from the Variscan of the French Massif Central.

In southern Tibet, Burchfiel *et al.* (1992) have shown that N-vergent *S–C* mylonite fabrics indicate that the low-angle N-dipping contact between the Greater Himalayan and Tibetan sedimentary sequences is a major normal fault—the South Tibetan Detachment System. This extensional interpretation is supported by such observations as: (1) the fault places Paleozoic or Mesozoic rocks onto Cambrian or Precambrian (?) footwall lithologies; (2) the hangingwall lithologies contain greenschist-facies mineral assemblages while the footwall assemblages are indicative of middle–upper amphibolite-facies; and (3) the footwall shows evidence for the progressive development of N-vergent ductile–brittle extensional structures. Burchfiel *et al.* (1992) have argued that since the presence of gently dipping normal faults that parallel thrust faults in the same mountain range can be documented in the Himalayas, it is possible that similar structures, which have previously been mapped as thrust faults, may also be present in other mountain ranges. We believe that the southern flank of the Brooks Range may be one such example.

CONCLUSIONS

Within the Florence and Fall Creeks area of the south-central Brooks Range, a series of weakly metamorphosed greywackes and phyllites (the MP unit) structurally overlie higher grade basement rocks of the Brooks Range Schist Belt. The contact between these two S-dipping tectonic units is referred to as the Florence Creek Fault. Microstructural and petrofabric analysis of quartz-rich horizons within both tectonic units leads to the following conclusions.

(1) A dominant top-down-to-the-south shear sense is indicated by the observed obliquity between foliation and alignment (S_B) of elongate dynamically recrystallized quartz grains. This inferred shear sense is independently supported by the observed quartz *c*-axis fabric asymmetry in the same samples and is in direct conflict with previous workers who have attributed foliation development on the southern flank of the Brooks Range to N-directed thrusting.

(2) The tectonic juxtaposition of low-grade metamorphic rocks of the MP unit above higher grade rocks of the underlying Schist Belt suggests that this penetrative top-down-to-the-south deformation is of extensional origin. A backthrust interpretation of these relationships seems unlikely as low-grade rocks structurally overlie higher grade rocks along the entire length (>500 km) of the southern Brooks Range.

(3) Within the Schist Belt rocks, a top-down-to-the-south shear sense has been found in samples collected at estimated distances ranging from less than 100 m beneath the projected position of the Florence Creek Fault, to approximately 7.7 km beneath the fault. In the overlying MP unit, a top-down-to-the-south shear sense has been found in quartz veins located at distances of between 50 and 400 m above the fault.

(4) These observations indicate that the Florence and Fall Creeks area may be situated over a large scale (at least 8.0 km thick) zone of extensional shear dipping towards the south. How far this zone of penetrative deformation can be traced along strike remains unclear.

Acknowledgements—Fieldwork for this study was funded by a grant from ARCO Alaska to Miller, and made possible by helicopter and logistical support from the Trans-Alaska Crustal Transect Geologic Studies Project of the U.S. Geological Survey headed by T. E. Moore and W. J. Nokleberg during the summers of 1989 and 1990. R. D. Law particularly wishes to thank Richard Gottschalk for generously supplying unpublished data, Dianna Solie of the Alaska Division of Geological and Geophysical Surveys for her hospitality during fieldwork and Delpfine Welch for advice on computer programs. Laboratory work and preparation of data for publication was supported by National Science Foundation Grants EAR-9018929 to R. D. Law and EAR-9018922 to E. L. Miller. Critical reviews by J. Gilotti, R. R. Gottschalk, J. W. Handschy, D. Solie and S. F. Wojtal substantially improved the manuscript and are gratefully acknowledged.

REFERENCES

Armstrong, R. L., Harakal, J. E., Forbes, R. B., Evans, B. W. & Thurston, S. P. 1986. Rb–SR and K–AR study of metamorphic rocks of the Seaward Peninsula and southern Brooks Range, Alaska. In: *Blueschist and Eclogites* (edited by Evans, B. W. & Brown, E. H.). *Mem. geol. Soc. Am.* **164**, 185–203.

Ave Lallement, H. G., Oldow, J. S. & Gottschalk, R. R. 1989. Mesoscopic fault analysis in the south-central Brooks Range fold and thrust belt, Alaska. *Geol. Soc. Am. Abs. w. Prog.* **21**, 52.

Behrmann, J. H. & Platt, J. P. 1982. Sense of nappe emplacement from quartz *c*-axis fabrics: an example from the Betic Cordilleras (Spain). *Earth Planet. Sci. Lett.* **59**, 208–215.

Behrmann, J. H. & Ratschbacher, L. 1989. Archimedes revisited: a structural test of eclogite emplacement models in the Austrian Alps. *Terra Nova* **1**, 242–252.

Bird, K. J. 1977. Late Paleozoic carbonates from the south-central Brooks Range. *U.S. geol. Surv. Circ.* **751-B**, B19–B20.

Bouchez, J.-L., Lister, G. S. & Nicolas, A. 1983. Fabric asymmetry and shear sense in movement zones. *Geol. Rdsch.* **72**, 401–419.

Box, S. E. 1987. Late Cretaceous or younger SW-directed extensional faulting: Cosmos Hills, Brooks Range, Alaska. *Geol. Soc. Am. Abs. w. Prog.* **19**, 212.

Brosge, W. P. & Reiser, H. N. 1971. Preliminary bedrock geologic map: Wiseman and eastern Survey Pass quadrangles, Alaska. *U.S. geol. Surv. Open-file Map* **479**, scale 1:250 000.

Brunel, M. & Chauvet, A. 1993. Devonian extension of the Caledonian crust of western Norway; quartz fabric evolution across the Sognefjord–Nordfjord shear zone. In: *Late Orogenic Extension in Mountain Belts* (edited by Sérrane, M. & Malavielle, J.). *Doc. Bur. Recher. Géol. Min. Fr.* **219**, 28–29.

Burchfiel, B. C., Zhiliang, C. K., Hodges, K. V., Yuping, L., Royden, L. H., Chagrong, D. & Jiene, X. 1992. The South Tibetan Detachment System, Himalayan Orogen: extension contemporaneous with and parallel to shortening in a collisional mountain belt. *Spec. Pap. geol. Soc. Am.* **269**.

Butler, R. W. H. 1984. Structural evolution of the Moine thrust belt between Loch More and Glendu, Sutherland. *Scott. J. Geol.* **20**, 161–179.

Chauvet, A. & Brunel, M. 1988. La grande faille normale ductile du Sunnfjord. Une extension NW-SE dans la chaîne calédonienne de l'Ouest Norvége. *C.r. Acad. Sci. Paris Ser.* II **307**, 415–422.

Christiansen, P. P. 1989. Structural, metamorphic and thermal evolution of the Cosmos Hills, northern Alaska. M.S. thesis, Stanford University, California.

Cobbold, P. R. & Quinquis, H. 1980. Development of sheath folds in shear regimes. *J. Struct. Geol.* **2**, 119–126.

Dell'Angelo, L. N. & Tullis, J. 1989. Fabric development in experimentally sheared quartzites. *Tectonophysics* **169**, 1–22.

Dewey, J. F. 1988. Extensional collapse of orogens. *Tectonics* **7**, 1123—1139.

Dillon, J. T. 1989. Structure and stratigraphy of the southern Brooks Range and northern Koyukuk basin near the Dalton Highway. In: *Dalton Highway, Yukon River to Prudoe Bay, Alaska, Bedrock Geology of the Eastern Koyukuk Basin, central Brooks Range, and east-central Arctic Slope* (edited by Mull, C. G. & Adams, K. E.). *Alaska Dept Nat. Res. Div. Geo:l Geophys. Surv. Guidebook* **7**, Vol. 2, 157–188.

Dillon, J. T., Brosge, W. P. & Dutro, J. T., Jr. 1986. Generalized geologic map of the Wiseman quadrangle, Alaska. *U.S. geol. Surv. Open-file Rep.* **OF 86-219**, scale 1:250 000.

Dillon, J. T., Hamilton, W. B. & Lueck, L. L. 1981. Geologic map of the Wiseman A-3 quadrangle, Alaska. *Alaska Div. Geol. Geophys. Surv. Open-file Rep.* **119**, 1 sheet, scale 1:63 360.

Dillon, J. T., Pessel, G. H., Chen, G. H. & Veach, N. C. 1980. Middle Paleozoic magmatism and orogenesis in the Brooks Range, Alaska. *Geology* **8**, 338–343.

Dillon, J. T., Pessel, G. H., Lueck, L. L. & Hamilton, W. B. 1987. Geologic map of the Wiseman A-4 quadrangle, south-central Brooks range, Alaska. *Alaska Div. Geol. Geophys. Surv. Prof. Rep.* **87**, 2 sheets, scale 1:63 360.

Dusel-Bacon, C., Brosge, W. P., Till, A. B., Fitch, M. R., Mayfield, C. F., Reiser, H. N. & Miller, T. P. 1989. Distribution, facies, ages and proposed tectonic associations of regionally metamorphosed rocks in northern Alaska. *Prof. Pap. U.S. geol. Surv.* **1497A**.

Etchecopar, A. & Vasseur, G. 1987. A 3-D kinematic model of fabric development in polycrystalline aggregates: comparisons with experimental and natural examples. *J. Struct. Geol.* **9**, 705–718.

Gottschalk, R. R. 1987. Structural and petrologic evolution of the south-central Brooks Range, Alaska. Unpublished Ph.D. dissertation, Rice University, Houston, Texas.

Gottschalk, R. R. 1990. Structural evolution of the Schist Belt, south-central Brooks Range fold and thrust belt. *J. Struct. Geol.* **12**, 453–469.

Gottschalk, R. R., Ave Lallement, H. G. & Oldow, J. S. 1990. ^{40}Ar/^{39}Ar thermochronology of metamorphic rocks in the south-central Brooks Range fold and thrust belt, Alaska. *Geol. Soc. Am. Abs. w. Prog.* **22**, A326.

Gottschalk, R. R. & Oldow, J. S. 1988. Low angle normal faults in the south-central Brooks Range fold and thrust belt, Alaska. *Geology* **16**, 395–399.

Grantz, A., Moore, T. E. & Roeske, S. 1991. Continental–ocean transect A-3: Gulf of Alaska to Arctic Ocean. *Geol. Soc. Am. Centenniel Continent/Ocean Transect Ser.* 3 sheets, scale 1:500 000.

Green, H. W., Griggs, D. T., & Christie, J. M. 1970. Syntectonic recrystallisation and annealing of quartz aggregates. In: *Experimental and Natural Rock Deformation* (edited by Paulitsch, P.). Springer, Berlin, 272–335.

Hanmer, S. H. & Passchier, C. 1991. Shear-sense indicators: a review. *Geol. Surv. Can. Pap.* **90–17**.

Hitzman, M. W., Profett, J. M. & Schmidt, S. 1986. Geology and mineralization of the Ambler District. *Econ. Geol.* **91**, 1592–1618.

Hobbs, B. E. 1985. The geological significance of microfabric analysis. In: *Preferred Orientations in Deformed Metals and rocks: An Introduction to Modern Texture Analysis* (edited by Wenk, H.-R.). Academic Press, Orlando, 463–484.

Hodges, K. V. & Walker, J. D. 1992. Extension in the Cretaceous Sevier orogen, North American Cordillera. *Bull. geol. Soc. Am.* **104**, 560–569.

Hsu, K. J. 1992. Reply on "Exhumation of high-pressure metamorphic rocks". *Geology* **20**, 186.

Jessell, M. W. 1988. Simulation of fabric development in recrystallizing aggregates—II. example model runs. *J. Struct. Geol.* **10**, 779–794.

Jessell, M. W. & Lister, G. S. 1990. A simulation of the temperature dependence of quartz fabrics. In: *Deformation Mechanisms, Rheology and Tectonics* (edited by Knipe, R. J. & Rutter, E. H.). *Spec. Publs geol. Soc. Lond.* **54**, 353–362.

Jones, D. L., Coney, P. J., Harms, T. A. & Dillon, J. T. 1988. Interpretive geologic map and supporting radiolarian data from the Angayucham terrane, Coldfoot area, southern Brooks Range, Alaska. *U.S. geol. Surv. Misc. Field Studies Map* **MF-1993**, scale 1:63 360.

Knipe, R. J. & Law, R. D. 1987. The influence of crystallographic orientation and grain boundary migration on microstructural and textural evolution in a *S–C* mylonite. *Tectonophysics* **135**, 155–169.

Krohe, A. 1987. Kinematics of Cretaceous nappe tectonics in the Austroalpine basement of the Koralpe region (eastern Austria). *Tectonophysics* **136**, 171–196.

Law, R. D. 1987. Heterogeneous deformation and quartz crystallographic fabric transitions: natural examples from the Stack of Glencoul, northern Assynt. *J. Struct. Geol.* **9**, 819–833.

Law, R. D. 1990. Crystallographic fabrics: a selective review of their applications to research in structural geology. In: *Deformation Mechanisms, Rheology and Tectonics* (edited by Knipe, R. J. & Rutter, E. H.). *Spec. Publs geol. Soc. Lond.* **54**, 335–352.

Law, R. D., Casey, M. & Knipe, R. J. 1986. Kinematic and tectonic significance of microstructures and crystallographic fabrics within quartz mylonites from the Assynt and Eriboll areas of the Moine thrust zone, NW Scotland. *Trans. R. Soc. Edinb., Earth Sci.* **77**, 99–123.

Law, R. D., Knipe, R. J. & Dayan, H. 1984. Strain path partitioning within thrust sheets: microstructural and petrofabric evidence from the Moine thrust zone at Loch Eriboll, northwest Scotland. *J. Struct. Geol.* **6**, 477–497.

Lee, J. F., Miller, E. M. & Sutter, J. F. 1987. Ductile strain and metamorphism in an extensional tectonic setting: a case study from the northern Snake Range, Nevada, USA. In: *Continental Extension Tectonics* (edited by Coward, M. P., Dewey, J. F. & Hancock, P. L.). *Spec. Publs geol. Soc. Lond.* **28**, 267–298.

Lister, G. S. 1977. Discussion: Crossed girdle c-axis fabrics in quartzites plastically deformed by plane strain and in progressive simple shear. *Tectonophysics* **39**, 51–54.

Lister, G. S. & Hobbs, B. E. 1980. The simulation of fabric development during plastic deformation, the effects of deformation history. *J. Struct. Geol.* **2**, 355–370.

Lister, G. S. & Snoke, A. 1984. S–C mylonites. *J. Struct. Geol.* **6**, 617–638.

Lister, G. & Williams, P. F. 1979. Fabric development in shear zones, theoretical controls and observed phenomena. *J. Struct. Geol.* **1**, 283–297.

Little, T. A., Miller, E. L., Lee, J. & Law, R. D. 1994. Extensional origin of ductile fabrics in the Schist Belt, Central Brooks Range, Alaska—I. Geologic and structural studies. *J. Struct. Geol.* **16**.

Malavieille, J. 1993. Late orogenic extension in mountain belts: insights from the Basin and Range and the late Paleozoic Variscan Belt. *Tectonics* **12**, 1115–1130.

Malavieille, J., Guihot, P., Costa, S., Lardeaux, J. M. & Gardien, V. 1990. Collapse of the thickened Variscan crust in the French Massif Central: Mont Pilat extensional shear zone and St. Etienne Late Carboniferous basin. *Tectonophysics* **177**, 139–149.

Mayfield, C. G., Tailleur, I. L. & Ellersieck, I. 1988. Stratigraphy, structure and palinspastic syntheses of the western Brooks Range, northwestern Alaska. *Prof. Pap. U.S. geol. Surv.* **1399**, 143–186.

Means, W. D. 1981. The concept of steady-state foliation. *Tectonophysics* **78**, 179–199.

Michard, A., Chopin, C. & Henry, C. 1993. Compression versus extension in the exhumation of the Dora-Maira coesite-bearing unit, Western Alps, Italy. *Tectonophysics* **221**, 173–193.

Miller, E. L. 1987. Dismemberment of the Brooks Range orogenic belt during middle Cretaceous extension. *Geol. Soc. Am. Abs. w. Prog.* **19**, 432.

Miller, E. L., Christiansen, P. P. & Little, T. A. 1990a. Structural studies in the southernmost Brooks Range, Alaska. *Geol. Ass. Can. Prog. w. Abs.* **15**, A89.

Miller, E. L. & Hudson, T. A. 1991. Mid-Cretaceous extensional fragmentation of a Jurassic–Early Cretaceous compressional orogen, Alaska. *Tectonics* **10**, 781–796.

Miller, E. L. & Hudson, T. A. 1993. Reply: "Mid-Cretaceous fragmentation of a Jurassic–Early Cretaceous compressional orogen, Alaska" *Tectonics* **12**, 1082–1086.

Miller, E. L., Law, R. D. & Little, T. A. 1990b. Evidence for extensional deformation on the southern flank of the Brooks Range in the Florence Creek area, Wiseman A-3 quadrangle, Alaska. *Geol. Soc. Am. Abs. w. Prog.* **22**, A183.

Molnar, P. & Lyon-Caen, H. 1988. Some simple physical aspects of the support, structure and evolution of mountain belts. In: *Processes in Continental Lithospheric Deformation* (edited by Clark, S. P., Burchfiel, B. C. & Suppe, J.). *Spec. Pap. geol. Soc. Am.* **218**, 179–208.

Mull, C. G., Roeder, D. H., Tailleur, I. L., Pessel, G. H., Grantz, A. & May, S. D. 1987. Geologic sections and maps across the Brooks Range and Arctic slope to Beaufort Sea, Alaska. *Geol. Soc. Am. Map & Chart Series* **MC-28S**.

Murphy, J. M. & Patton, W. W. 1988. Geologic setting and petrography of the phyllite and metagreywacke thrust panel, north-central Alaska. *U.S. geol. Surv. Circ.* **1016**, 104–108.

Nelson, S. W. & Grybeck, D. 1980. Metamorphic rocks of the Survey Pass quadrangle, Brooks Range, Alaska. *U.S. geol. Surv. Misc. Field Studies Map* **MF 1176-C**, scale 1:250 000.

Nilsen, T. 1989. Stratigraphy and sedimentology of Cretaceous sedimentary rocks, Yukon–Koyukuk Basin, west central Alaska. *J. geophys. Res.* **94**, 15 925–15 940.

Norton, M. G. 1986. Late Caledonian extension in western Norway: a response to extreme crustal thickening. *Tectonics* **5**, 195–204.

Norton, M. G. 1987. The Nordfjord-Sogn Detachment, W. Norway. *Norsk geol. Tidsskr.* **67**, 93–106.

Norton, M. G., McClay, K. R. & Way, N. A. 1987. Tectonic evolution of Devonian basins in northern Scotland and southern Norway. *Norsk geol. Tidsskr.* **67**, 323–338.

Oldow, J. S., Ave Lallement, H. G., Gottschalk, R. R. & Snee, L. W. 1991. Timing and kinematics of Cretaceous contraction and extension in the southern Brooks Range, Alaska. *Eos* **72**, 295.

Oldow, J. S., Seidensticker, C. M., Phelps, J. C., Julian, F. E., Gottschalk, R. R., Boler, K. W., Handschy, J. W. & Ave Lallement, H. G. 1987. Balanced cross-sections through the central Brooks Range and North Slope, Arctic Alaska. Eight plates, American Association of Petroleum Geologists, Tulsa, Okla.

Patton, W. W. & Box, S. E. 1989. Tectonic setting of the Yukon–Koyukuk basin and its borderlands, western Alaska. *J. geophys. Res.* **94**, 15 807–15 820.

Pavlis, T. L. Sisson, B. S., Foster, H. L., Nokleberg, W. J. & Plafker, G. 1993. Mid-Cretaceous extensional tectonics of the Yukon–Tanana Terrane, Trans-Alaska Crustal Transect (TACT), east-central Alaska. *Tectonics* **12**, 103–122.

Platt, J. P. 1986. Dynamics of orogenic wedges and the uplift of high-pressure metamorphic rocks. *Bull. geol. Soc. Am.* **97**, 1037–1053.

Platt, J. P. 1987. The uplift of high-pressure–low-temperature metamorphic rocks. *Phil. Trans. R. Soc. Lond.* **A321**, 87–103.

Platt, J. P. 1992. Comment on "Exhumation of high-pressure metamorphic rocks". *Geology* **20**, 186–187.

Platt, J. P. & Behrmann, J. H. 1986. Structures and fabrics in a crustal scale shear zone, Betic Cordilleras, SE Spain. *J. Struct. Geol.* **8**, 15–34.

Powell, D. & Glendinning, N. R. W. 1990. Late Caledonian extensional reactivation of a ductile thrust in NW Scotland. *J. geol. Soc. Lond.* **147**, 979–987.

Price, G. P. 1985. Preferred orientations in quartzites. In: *Preferred Orientations in Deformed Metals and Rocks: An Introduction to Modern Texture Analysis* (edited by Wenk, H.-R.). Academic Press, Orlando, 385–406.

Ramsay, J. G. 1967. *Folding and Fracturing of Rocks.* McGraw Hill, New York.

Ramsay, J. G., Casey, M. & Kligfield, R. 1983. Role of shear in development of the Helvetic fold-thrust belt of Switzerland. *Geology* **11**, 439–442.

Ratschbacher, L., Frisch, W., Neubauer, F., Schmidt, S. M. &

Neugebauer, J. 1989. Extension in compressional belts: the Eastern Alps. *Geology* **17**, 404–407.

Schmid, S. M. & Casey, M. 1986. Complete fabric analysis of some commonly observed quartz c-axis patterns. In: *Mineral and Rock Deformation; Laboratory Studies—The Paterson Volume* (edited by Hobbs, B. E. & Heard, H. C.). *Am. Geophys. Un. Geophys. Monogr.* **36**, 263–286.

Séranne, M. & Séguret, M. 1987. The Devonian basins of western Norway: tectonics and kinematics of an extending crust. In: *Continental Extension Tectonics* (edited by Coward, M. P., Dewey, J. F. & Hancock, P. L.). *Spec. Publs geol. Soc. Lond.* **28**, 537–548.

Simpson, C. 1986. Determination of movement sense in mylonites. *J. geol. Educ.* **34**, 246–261.

Simpson, C. & Schmid, S. M. 1983. An evaluation of criteria to deduce the sense of movement in sheared rocks. *Bull. geol. Soc. Am.* **94**, 1281–1288.

Starkey, J. 1977. The contouring of orientation data represented in spherical projection. *Can. J. Earth Sci.* **14**, 268–277.

Starkey, J. 1989. *Microcomputer Workshop: Quantitative Petrofabric Analysis*. 9th Annual Meeting, Structural Geology & Tectonics Division, Geological Association of Canada. London, Ontario, Canada.

Starkey, J. & Cutforth, C. 1978. A demonstration of the interdependence of the degree of quartz preferred orientation and the quartz content of deformed rocks. *Can. J. Earth Sci.* **15**, 841–847.

Till, A. B., Box, S. E., Roeske, S. M. & Papperton, W. W. 1993. Comment on "Mid-Cretaceous fragmentation of a Jurassic–Early Cretaceous compressional orogen, Alaska" by E. L. Miller and T. L. Hudson. *Tectonics* **12**, 1076–1081.

Till, A. B. & Moore, T. E. 1991. Tectonic relations of the Schist Belt, southern Brooks Range, Alaska. *Eos* **72**, 295.

Till, A. B., Schmidt, J. M. & Nelson, S. W. 1988. Thrust involvement of metamorphic rocks, southwestern Brooks Range, Alaska. *Geology* **16**, 930–933.

Tullis, J. 1977. Preferred orientation of quartz produced by slip during plane strain. *Tectonophysics* **39**, 87–102.

Tullis, J., Christie, J. M. & Griggs, D. T. 1973. Microstructures and preferred orientations of experimentally deformed quartzites. *Bull. geol. Soc. Am.* **84**, 297–314.

Wenk, H.-R., Canova, G., Molinari, A. & Kocks, U. P. 1989. Viscoplastic modeling of texture development in quartzite. *J. geophys. Res.*, **94**, 17,895–17,906.

Wenk, H.-R. & Christie, J. M. 1991. Review paper—Comments on the interpretation of deformation textures in rocks. *J. Struct. Geol.* **13**, 1091–1110.

Wheeler, J. 1991. Structural evolution of a subducted continental sliver: the northern Dora Maira massif, Italian Alps. *J. geol. Soc. Lond.* **148**, 1101–1113.

Wheeler, J. & Butler, R. W. H. 1993. Evidence for extension in the western Alpine Orogen: the contact between the oceanic Piemonte and overlying continental Sesia units. *Earth Planet. Sci. Lett.* **117**, 457–474.

Wilber, S. C., Siok, J. P. & Mull, C. G. 1987. A comparison of two petrographic suites of the Okpikruak Formation: A point-count analysis. In: *Alaskan North Slope Geology, Volume 1* (edited by Tailleur, I. & Weimer, P.). *Spec. Publs Pacific Section, Soc. econ. Paleont. Miner., Bakersfield, Calif.*, 441–447.